

REGULATION OF *TRYPANOSOMA CRUZI* S-ADENOSYLMETHIONINE
DECARBOXYLASE ACTIVITY

APPROVED BY SUPERVISORY COMMITTEE

Meg Phillips, Ph.D.

Phil Thomas, Ph.D.

Joe Albanesi, Ph.D.

Melanie Cobb, Ph.D.

DEDICATION

To my family for the love, support and encouragement they have given me throughout my entire life, especially during my years in graduate school.

REGULATION OF *TRYPANOSOMA CRUZI* S-ADENOSYLMETHIONINE
DECARBOXYLASE ACTIVITY

By

TRACY CLYNE BESWICK

DISSERTATION

Presented to the Faculty of the Graduate School of Biomedical Sciences

The University of Texas Southwestern Medical Center at Dallas

In Partial Fulfillment of the Requirements

For the Degree of

DOCTOR OF PHILOSOPHY

The University of Texas Southwestern Medical Center at Dallas
Dallas, Texas
Dec, 2005

Copyright

By

TRACY CLYNE BESWICK 2005

All Rights Reserved

REGULATION OF *TRYPANOSOMA CRUZI* S-ADENOSYLMETHIONINE
DECARBOXYLASE ACTIVITY

TRACY CLYNE BESWICK, Ph.D.

The University of Texas Southwestern Medical Center at Dallas, 2005

MENTOR: MARGARET A. PHILLIPS, Ph.D.

Chagas' disease, caused by *Trypanosoma cruzi*, is a major health problem for which there is no good chemotherapy. Development of new drugs is crucial. One strategy is to develop inhibitors of enzymes in essential metabolic pathways. Trypanosomes need polyamines to survive; thus, the enzymes in the polyamine biosynthetic pathway are targets for drug development. Characterization of S-adenosylmethionine decarboxylase (the rate-limiting enzyme in the pathway)

activity in trypanosomes and comparison to human AdoMetDC will aid the discovery of novel, species specific inhibitors.

I have characterized putrescine stimulation of *T. cruzi* AdoMetDC activity as well as the allostery between the putrescine binding site and the active site of the enzyme. Putrescine is capable of stimulating *T. cruzi* AdoMetDC decarboxylation but not proenzyme processing. This contrasts with the human enzyme, for which processing and decarboxylation are both modestly stimulated by putrescine. R13, a Leu in the human enzyme, was shown to be essential for processing in the *T. cruzi* enzyme. Additionally, D174 is an important binding determinant for putrescine in both species of AdoMetDC. Other mutations near the putative putrescine site (S111R and F285H) indicate that the putrescine binding site for *T. cruzi* AdoMet DC is more surface-exposed than the human enzyme.

Putrescine stimulates decarboxylase activity 41 fold for *T. cruzi* AdoMetDC (compared to 1.7 fold for the human enzyme). This stimulation is achieved through allosteric binding to a site approximately 15 Å away from the active site. To examine this allostery, we used putrescine and active site mutations as well as an active site inhibitor, CGP 40215. This inhibitor unexpectedly exhibited noncompetitive inhibition with a K_i of 32μM and 3μM in the absence and presence of putrescine, respectively (K_i for the human enzyme is 10nM and 6nM). Residues important for communication between the two sites

include L221, H5, D174, S111 and F285. L221, a Thr residue in the human enzyme, is partially responsible for some of the species specificity as the K_i for L221T was 800nM. The differences in putrescine stimulation and CGP 40215 inhibition indicate development of species specific inhibitors is possible and could be an effective strategy for novel antitrypanosomal chemotherapy.

TABLE OF CONTENTS

Title- Fly.....	i
Dedication.....	ii
Title Page.....	iii
Copyright.....	iv
Abstract.....	v
Table of Contents.....	vii
List of Figures.....	xii
List of Schemes and Tables.....	xiii
List of Abbreviations.....	xiv
 Chapter 1	
Introduction.....	1
A. Trypanosomiasis.....	1
1. Overview.....	1
2. South American Trypanosomiasis.....	1
3. African Trypanosomiasis.....	3
B. Polyamines.....	4
1. Polyamine Structure.....	4
2. Polyamine Function.....	5
3. Polyamine Homeostasis and the Polyamine Biosynthetic Pathway.....	5
4. Polyamine Enzymes as Drug Targets.....	6
5. Polyamines in Trypanosomes.....	6
C. S-Adenosylmethionine Decarboxylase.....	7

1. Enzyme Processing and Cofactor Formation.....	7
2. Enzyme Biochemistry and Mechanism.....	8
3. Enzyme Structure.....	10
4. AdoMetDC Inhibitor Studies.....	12

Chapter 2

Mechanism of Putrescine Stimulation of <i>T. cruzi</i> AdoMetDC.....	22
A. Introduction.....	22
B. Experimental Procedures.....	23
1. Materials.....	23
2. Expression and Purification of <i>T. cruzi</i> AdoMetDC.....	24
3. Human AdoMetDC cloning and expression.....	24
4. Site-directed Mutagenesis of <i>T. cruzi</i> AdoMetDC.....	25
5. <i>In vitro</i> Translation and Proenzyme Processing.....	25
6. Analytical Ultracentrifugation.....	25
7. Cyanoborohydride Reduction of the Substrate and Activator.....	26
8. Putrescine Binding Assays.....	27
9. Steady State Kinetic Analysis.....	28
C. Results.....	28
1. Effects of Putrescine on Autocatalytic Processing of <i>T. cruzi</i> AdoMetDC.....	29
2. Analysis of Schiff Base Intermediates Formed with <i>T. cruzi</i> AdoMetDC by Trapping with Cyanoborohydride.....	30
3. Analysis of the Oligomeric State of <i>T. cruzi</i> AdoMetDC by Equilibrium Sedimentation.....	30
4. Assessment of Putrescine Binding to <i>T. cruzi</i> AdoMetDC by Fluorescence and by Ultrafiltration.....	31
5. Putrescine Binding to Human AdoMetDC.....	32
6. Site-Directed Mutagenesis of Putative Putrescine Binding Site Residues.....	33
D. Discussion.....	35

Chapter 3

Mechanism of drug selectivity of AdoMetDC using inhibitors CGP 40215 and CGP 48664.....	47
A. Introduction.....	47

B. Experimental procedures.....	48
1. Materials.....	48
2. Expression and Purification of AdoMetDC.....	48
3. Site-directed Mutagenesis of <i>T. cruzi</i> AdoMetDC.....	49
4. Steady State Kinetic Analysis.....	49
5. Putrescine Activation.....	49
6. IC ₅₀ Determination.....	50
C. Results.....	50
1. Wild-type <i>T. cruzi</i> AdoMetDC kinetics, putrescine stimulation, and inhibition by CGP 40215.....	50
2. Human AdoMetDC kinetics and inhibition by CGP 40215.....	51
3. Analysis of putrescine binding mutants.....	53
4. Analysis of active site mutations.....	55
5. CGP 48664 inhibition of various AdoMetDCs.....	56
D. Discussion.....	58
 Chapter 4	
Yeast complementation/selection with inhibitors using mutated <i>T. cruzi</i> AdoMetDC.....	74
A. Introduction.....	74
B. Experimental Procedures.....	75
1. Yeast Strains.....	75
2. Cloning of <i>T. cruzi</i> and human AdoMetDC genes into yeast expression vector.....	75
3. Determination of IC ₅₀ value for CGP 40215.....	76
4. Transformation of the <i>T. cruzi</i> AdoMetDC yeast vector into $\Delta spe2$ cells.....	76
5. Growth of transformants on minimal media.....	77
C. Results and Discussion.....	77
1. Cloning of <i>T. cruzi</i> AdoMetDC gene into yeast expression vectors...77	
2. Determination of IC ₅₀ value of CGP 40215 for <i>T. cruzi</i> AdoMetDC...78	
3. Growth of transformants on YNBGal-P-ura plates.....79	
References.....	83

Vita.....	89
-----------	----

PRIOR PUBLICATIONS

1. Tlapak-Simmons VL, Baggenstoss BA, Clyne T, Weigel PH (1999) Purification and lipid dependence of the recombinant hyaluronan synthases from *Streptococcus pyogenes* and *Streptococcus equisimilis*, *Journal of Biological Chemistry*, **274**, pp. 4239-45.
2. Clyne T, Kinch LN, Phillips MA (2002) Putrescine activation of *Trypanosoma cruzi* S-adenosylmethionine decarboxylase, *Biochemistry*, **44**, pp.13207-16.

LIST OF FIGURES

FIGURE 1.1	Polyamine biosynthetic pathway.....	15
FIGURE 1.2	Proposed processing reaction mechanism for AdoMetDC.....	16
FIGURE 1.3	Decarboxylation of AdoMet.....	17
FIGURE 1.4	AdoMetDC sequence alignment for <i>T. cruzi</i> , potato and human enzymes.....	18
FIGURE 1.5	Structure of putrescine and active sites of human AdoMetDC.....	19
FIGURE 1.6	Structures of AdoMetDC inhibitors.....	20
FIGURE 2.1	Structure of Human AdoMetDC putrescine binding site.....	39
FIGURE 2.2	Proenzyme processing of <i>T. cruzi</i> and human AdoMetDC.....	40
FIGURE 2.3	Analysis of Schiff base intermediates formed with <i>T. cruzi</i> AdoMetDC.....	41
FIGURE 2.4	Sedimentation equilibrium analysis of <i>T. cruzi</i> AdoMetDC.....	42
FIGURE 2.5	Analysis of putrescine binding to <i>T. cruzi</i> AdoMetDC by intrinsic fluorescence emission.....	43
FIGURE 2.6	Scatchard analysis of radiolabeled putrescine binding.....	44
FIGURE 3.1	Overlay of putrescine binding site of human and potato AdoMetDC structures.....	62
FIGURE 3.2	Active site of human AdoMetDC (cyan) with the inhibitor CGP 48664 (purple) complexed.....	63
FIGURE 3.3	Substrate titration wild type <i>T. cruzi</i> AdoMetDC.....	64
FIGURE 3.4	Putrescine titration of 1 μ M <i>T. cruzi</i> AdoMetDC with 32 μ M radioactive AdoMet.....	65
FIGURE 3.5	IC ₅₀ data for wild type <i>T. cruzi</i> AdoMetDC.....	66
FIGURE 3.6	IC ₅₀ data for human AdoMetDC.....	67
FIGURE 3.7	CGP 48664 dose response curve for wild type, E247A and D174V <i>T. cruzi</i> AdoMetDC	68
FIGURE 4.1	Schematic of the proposed <i>T. cruzi</i> AdoMetDC yeast selection using inhibitor CGP 40215 and a Δ <i>spe2</i> yeast strain.....	72

LIST OF TABLES

TABLE 1.1	Kinetic parameters for various AdoMetDCs in the presence of putrescine.....	36
TABLE 2.1	<i>T. cruzi</i> and Plant Amino Acid substitutions Identified in the Putrescine Binding Site of Human AdoMetDC.....	45
TABLE 2.2	Summary of Putrescine Binding and Kinetic Analysis of Wild-type and Mutant <i>T. cruzi</i> AdoMetDC.....	46
TABLE 3.1	Summary of previously determined and new data on activity of human and <i>T. cruzi</i> AdoMetDCs in the presence and absence of putrescine.....	70
TABLE 3.2	CGP 40215 Ki values for human and <i>T. cruzi</i> AdoMetDC.....	71
TABLE 3.3	Kinetic parameters for wild type and putrescine binding mutants of <i>T. cruzi</i> AdoMetDC.....	72
TABLE 3.4	Kinetic data for wild type and active site mutations of <i>T. cruzi</i> AdoMetDC.....	73

LIST OF ABBREVIATIONS

Å	angstrom
AdoMet	S-Adenosylmethionine
AdoMetDC	S-Adenosylmethionine decarboxylase
AMA	S-(5'-deoxy-5'-adenosyl)methylthioethylhydroxylamine
ATCC	American Tissue and Culture Collection
cm	centimeter
dc AdoMet	decarboxylated s-adenosylmethionine
DFMO	di-fluoromethylornithine
DNA	deoxyribonucleic acid
g	gram
H-bond	hydrogen bond
hr	hour
kDa	kilodalton
kg	kilogram
L	liter
LB	Luria Bertani media
M	molar
MAOEA	5'-deoxy-5'-[(2-aminooxyethyl)-methylamino]adenosine
MGBG	methylglyoxal bis(guanyl)hydrazone
MHZPA	5'-deoxy-5''-[(3-hydrazino-propyl)methylamino]adenosine
min	minute
ml	milliliter
mM	millimolar
µg	microgram
µl	microliter
µM	micromolar
NIH	National Institute of Health
nm	nanometer
nM	nanomolar
OD280	optical density at 280 nm
ODC	ornithine decarboxylase
PCR	polymerase chain reaction
PDB	protein data bank
PLP	pyridoxyl phosphate
Pmol	picomoles
PMSF	phenylmethylsulfonyl fluoride
Pvl	pyruvoyl
RNA	ribonucleic acid
rpm	revolutions per minute

s	second
SDS-PAGE	sodium dodecyl sulfate polyacrylamide gel electrophoresis
TCA	trichloroacetic acid
UV	ultraviolet
VSG	variant surface glycoprotein

Chapter 1

Introduction

A. Trypanosomiasis

1. Overview

Trypanosomiasis exists in two varieties: African, which affects most of Africa and is referred to as Sleeping Sickness, and American, which afflicts Central and South America and is called Chagas' disease. Both diseases are caused by single-celled eukaryotic parasites called trypanosomes. The trypanosome life cycle starts inside an insect host, who transmits the parasite to a mammalian host. The cycle continues when the insect has a bloodmeal from an infected host. Trypanosomes have a special mechanism by which they evade the host's immune system. An antigen called variant surface glycoprotein (VSG) is exposed on the outer membrane of the trypanosome. Trypanosomes change the VSG that is expressed cyclically, approximately every two to three days. This confounds the host's immune response because by the time the host has developed antibodies to a VSG, the trypanosome is expressing a different one. Thus the host's immune system must start all over every two to three days (Barry and McCulloch 2001). This trickery makes it virtually impossible for the host to defend itself naturally, leaving the prospect of being cured up to chemotherapy. Trypanosomes pose a major health problem. Considering both diseases caused by trypanosomes, 16.3-18.5 million people are infected, with 180 million at risk (world health organization website). These diseases are detrimental on many levels, starting with individual health and escalating to social and economic effects. In short, trypanosomiasis is not only a 3rd world problem, it is a global burden. As such, it is imperative to develop new and effective drugs to treat these diseases.

2. South American Trypanosomiasis

T. cruzi is the causative agent of Chagas' disease, named for the doctor who first described it. *T. cruzi* is an intracellular parasite transmitted by the reduviid bug, commonly called a kissing bug because it prefers to bite people around the mouth. When it bites, it also defecates, and when the host scratches the bite, they unwittingly smear trypanosome-laden feces into the bite and thus become infected. Reduviid bugs live in cracks and crevices of poorly constructed houses, so the at-risk population is those who live in rural areas. The disease can also be transmitted by blood transfusion or congenitally from mother to fetus. Disease elimination efforts have been aimed at vector control, transfusion control and drug development.

As referred to above, the *T. cruzi* life cycle involves a host and a vector. When the vector has a bloodmeal from an infected host, the trypanosomes transform into epimastigotes once they reach the stomach and midgut of the insect. Epimastigotes attach to the walls of the rectal sac where they transform into metacyclic trypomastigotes. These are eliminated in feces. If the insect defecates on a host, the trypomastigotes can enter the host through breaks in the skin. The parasites transform into amastigotes in local host cells and multiply to release blood trypanosomes, which invade other tissues {Peluffo, 2004 #75}.

There are 2 stages of Chagas disease: acute and chronic. The acute phase refers to the month following initial exposure. It is characterized by generalized problems such as fever and swollen lymph nodes. Perhaps the most telltale sign of infection is Romana's sign (swelling around the site of parasite entry). Most patients, however, do not show any sign of infection during the acute stage. This is problematic because current chemotherapy for Chagas' disease is limited to the acute phase. The chronic stage of the disease begins as parasites invade cells of the host's organs, mainly the heart and intestines. This can take years, so most patients with Chagas live many years after their initial infection. 32% of cases are fatal because of megalocardia and megacolon. Historically there has been much

debate as to whether the chronic stage is due to actual parasites living in tissues or to the body's immune response to the trypanosomes. The current thought is that although there is clearly an anti-self response in the chronic stage, patients still benefit from a reduced parasite burden (Tarleton 2003). Thus it is recommended to administer antiparasitic treatments in the intermediary stage.

Current treatments for Chagas' disease are not appealing options. As mentioned above, there are no treatments available for the chronic stage, which is the most symptomatic. For the acute phase, benznidazole and nifurtimox are useful, although the side effects are severe and include peripheral neuropathy, seizures, skin rash, gastrointestinal disturbances, fatigue, headache, amnesia, and insomnia (PDR 2005). Nifurtimox kills trypanosomes through oxidative damage caused by free radical generation. Benznidazole's mechanism of action appears to be inhibiting protein and RNA synthesis (PDR 2005). Pathways that have been validated as drug targets include sterol biosynthesis, cruzi-pain mediated proteolysis and pyrophosphate metabolism (Urbina and Docampo 2003). Other possibilities include trypanothione synthesis and redox metabolism, dihydrofolate reductase, phospholipids biosynthesis and protein prenylation and acylation (Urbina and Docampo 2003).

3. African Trypanosomiasis

African trypanosomiasis exists in two forms: an acute form caused by *T. brucei rhodesiense* and a chronic form caused by *T. brucei gambiense*. *T.b.rhodesiense* typically affects southern and eastern Africa while *T.b.gambiense* is prevalent in central and western Africa. Both forms are transmitted by the Tsetse fly but can also be spread from mother to fetus and by blood transfusions.

There are two stages of infection. The first entails bouts of fever, headaches, pains in the joints and itching. The second stage involves neurological symptoms due to the parasites crossing the blood brain barrier. Symptoms of this

phase include confusion, sensory disturbances, poor coordination, and disturbances in the sleep cycle. The disease is fatal if untreated and permanent damage occurs if treatment is not given prior to the onset of the neurological phase.

Fortunately there are drug options for both phases of Sleeping Sickness, although a range of problems make these drugs far from ideal. Suramine and Pentamidine are capable of eliminating infections in the first stage for *T.b.rhodesiense* and *T.b.gambiense*, respectively. For late stage, melarsoprol and eflornithine are used. Melarsoprol, an arsenic derivative, is capable of curing both subtypes of the disease, although the side effects are severe and sometimes fatal. Resistance to Melarsoprol is on the rise, reaching 30% in some parts of central Africa. Eflornithine, also known as DFMO, is effective only against *T.b.gambiense*. DFMO is a suicide inhibitor of the enzyme ornithine decarboxylase (ODC), the first committed step in the polyamine biosynthetic pathway. It was first developed as an anti-cancer therapy but was ineffective because there is rapid turnover of human ODC. However, ODC in trypanosomes is not turned over rapidly, making DFMO lethal to these cells. Unfortunately, DFMO is not an ideal drug because the dosage is large and requires weeks of administering.

B. Polyamines

1. Polyamine structure

Polyamines are aliphatic amines that are positively charged at physiological pH. They are linear, flexible compounds in which the positive charges are separated by fixed distances. This molecular set up provides a unique opportunity to interact with negative charges and/or hydrophobic patches. Putrescine, spermidine and spermine (not found in trypanosomes) are the most common polyamines, although *T. cruzi* are able to uptake and use cadaverine.

2. Polyamine function

Polyamines are present in all cells at millimolar concentrations, although the free concentration of polyamines is likely very low due to the fact that most of them are bound to negatively-charged cellular components (Janne, Alhonen et al. 2004). They are involved in many cellular processes including growth and differentiation; DNA replication; RNA synthesis, translation and stabilization; and membrane transport (Morozova, Desmet et al. 1993). Gene deletions of polyamine biosynthetic enzymes in mice have shown that polyamines are involved in spermatogenesis, skin physiology, promotion of tumorigenesis and organ hypertrophy as well as neuronal protection (Janne, Alhonen et al. 2004). Transgenic activation of polyamine catabolic enzymes creates a complex phenotype affecting skin, female fertility, fat deposits, pancreatic activity and regenerative growth (Janne, Alhonen et al. 2004).

3. Polyamine homeostasis and the biosynthetic pathway

Polyamine homeostasis is achieved by regulating the biosynthetic anabolic and catabolic pathways as well as uptake. The polyamine biosynthetic pathway begins with 2 enzymes involved in parallel steps of the pathway, making them both rate-limiting enzymes for polyamine biosynthesis: ODC, and S-adenosylmethionine decarboxylase (AdoMetDC) (Voet 1995). ODC decarboxylates the amino acid ornithine to produce putrescine, the smallest polyamine. AdoMetDC decarboxylates S-adenosylmethionine (AdoMet) to give decarboxylated s-adenosylmethionine (dcAdoMet). The dcAdoMet is then used as an amino-propyl donor. Spermidine synthetase conjugates the amino-propyl to putrescine to make spermidine. Spermidine is elongated through amino-propylation catalyzed by spermine synthetase, giving rise to spermine. In humans and *T. cruzi*, putrescine stimulates the catalytic activity of AdoMetDC, whereas

plant AdoMetDCs are unaffected (Stanley and Pegg 1991; Schroder and Schroder 1995). Another point of interest is a unique function of polyamines in trypanosomes. While mammalian cells use glutathione to maintain redox balance, trypanosomes use trypanothione, a conjugate of spermidine to two glutathione molecules (Fairlamb and Cerami 1992). If trypanothione is not made by the cell, glutathione cannot rescue the trypanosome's normal redox balance, and the parasite dies. This unique aspect of trypanosomal polyamine usage strengthens the argument of using the polyamine biosynthetic pathway as a drug target for trypanosomes.

4. Polyamine enzymes as drug targets

As mentioned above, disruption of polyamine homeostasis has profound effects on cells and whole organisms. The biosynthetic pathway has been a drug target for cancer and parasitic diseases (Gerner and Meyskens 2004; Wallace and Fraser 2004). Initially developed to kill cancer cells, di-fluoromethylornithine (DFMO) was developed as a specific inhibitor of ornithine decarboxylase (ODC), the first enzyme in the polyamine biosynthetic pathway. Because mammalian ODC has such a rapid turnover rate, DFMO proved ineffective for fighting cancer. However, DFMO is curative for African Trypanosomiasis because *T. brucei*'s ODC has a slow turnover rate. This example shows that exploiting differences in polyamine metabolism between host and parasite is one way to combat trypanosomiasis.

5. Polyamines in Trypanosomes

T. cruzi has a robust transport system for the import of putrescine, spermidine, and AdoMet which allows these intracellular parasites to salvage host cell polyamines (Gonzalez, Ceriani et al. 1992). These trypanosomes lack ODC, making AdoMetDC the sole rate-limiting enzyme of the polyamine biosynthetic

pathway. Even though *T. cruzi* are capable of importing polyamines, it has been shown that lack of AdoMetDC activity reduces the ability of *T. cruzi* to infect host cells (Yakubu, Majumder et al. 1993). This could possibly be due to a build up of AdoMet. AdoMet, besides its involvement in polyamine synthesis, is the main source of methyl groups for all methylations the cell must perform. So, if there is an overabundance of AdoMet, it is likely that non-specific methylation could occur, which damages or kills the cell. Thus, AdoMetDC is a viable drug target for *T. cruzi*.

C. AdoMetDC

1. Enzyme Processing and Cofactor formation

Decarboxylases require a cofactor (typically PLP or pyruvate) as an electron sink to catalyze removal of the carboxyl group. AdoMetDC belongs to the family of decarboxylases that accomplish catalysis through a self-generated pyruvoyl cofactor. The other enzymes in this family include histidine decarboxylase and aspartate decarboxylase (van Poelje and Snell 1990). For AdoMetDC, the cofactor is formed on the N-terminus of the α subunit after the enzyme has undergone an autoserinolysis reaction, from here on referred to as the processing reaction. This reaction cleaves the enzyme into two subunits, α (32kD) and β (10kD) that remain closely associated after the cleavage has taken place. Both subunits are required for activity.

The reaction mechanism for AdoMetDC processing has been probed using mutagenesis and crystallographic studies in the human enzyme (Figure 1.2) (Stanley, Pegg et al. 1989; Xiong and Pegg 1999; Ekstrom, Tolbert et al. 2001; Tolbert, Zhang et al. 2003). In the proposed mechanism, Ser68 performs a nucleophilic attack on the backbone carbonyl of Glu67. According to structural data, there is no obvious base to abstract a proton from Ser68 to activate it. The

proposed method of activation is strain. Once the nucleophilic attack has occurred, an oxyoxazolidine intermediate is formed. After protonation by His243, an ester intermediate is formed. Abstraction from a proton on the C α carbon of Ser68 allows the ester bond to break, at which point the α and β subunits are made. Addition of water and subsequent removal of an amino group from the N-terminus of the α subunit creates the pyruvoyl group. Plant AdoMetDC enzymes process quickly and there is no need for putrescine(Xiong, Stanley et al. 1997). For human AdoMetDC, the processing reaction is stimulated by putrescine(Stanley and Pegg 1991). This occurs through a network of H-bonds involving residues Lys80, Glu11 and His243(Ekstrom, Tolbert et al. 2001). Mutation of human AdoMetDC residues Ser68, Ser229 and His243 prevent processing completely. Mutation at Cys82 still processes, although slowly and transamination often occurs, rendering the enzyme inactive(Stanley and Pegg 1991). Mutation E133Q will process only in the presence of putrescine. Putrescine is no longer capable of stimulating the processing reaction for mutants K80A, E11Q, D174N, E178Q and E256Q (Stanley and Pegg 1991; Stanley, Shantz et al. 1994).

2. Enzyme Biochemistry and Mechanism

AdoMetDC accomplishes catalysis through Schiff Base formation between the pyruvoyl cofactor and AdoMet (Figure 1.3). The resulting imine facilitates decarboxylation by participating as an electron sink for the carbanion produced upon removal of the carboxyl group. Once decarboxylation has occurred, the α carbon is protonated and the Schiff base is hydrolyzed, resulting in product release.

The most rigorous kinetic studies have been done on *T. cruzi* AdoMetDC, both in the presence and absence of putrescine (Kinch, Scott et al. 1999; Kinch

and Phillips 2000). In the absence of putrescine, k_{cat} is 0.007s^{-1} and K_{m} is 0.05mM . When saturating putrescine is added, k_{cat} is 0.06s^{-1} and K_{m} is 0.1mM , giving putrescine a 9 fold effect on activity. With single turnover analysis in the presence of putrescine, the apparent second order rate constant k_2/K_{s} is $3300\text{M}^{-1}\text{s}^{-1}$, putting a lower limit on k_{cat} at 6s^{-1} . Because single turnover measures the slowest step up to and including decarboxylation, this means the first half of the reaction is minimally 100 fold faster than product release (including Schiff base hydrolysis).

Kinetic parameters for AdoMetDCs from other species vary. The human enzyme has a k_{cat} of 0.481s^{-1} and a K_{m} of 0.078mM in 0.2mM putrescine (Stanley, Shantz et al. 1994). Similarly, AdoMetDC from *Saccharomyces cerevisiae* has a K_{m} of $90\mu\text{M}$ and k_{cat} of 0.9s^{-1} in the presence of saturating putrescine (Poso, Sinervirta et al. 1975). For most plant enzymes k_{cat} ranges from $3\text{-}46\text{s}^{-1}$ and K_{m} values range from $8\text{-}40\mu\text{M}$. Their activity is unaffected by putrescine (Choi and Cho 1994; Schroder and Schroder 1995; Park and Cho 1999).

Through mutagenesis studies, it is known that Cys82 plays a role in the acid/base chemistry required for Schiff base formation and likely hydrolysis (Kinch and Phillips 2000). E11, E133 and E256 are important for human AdoMetDC activity (Stanley and Pegg 1991). K80 is important for human AdoMetDC activity in the absence of putrescine (Stanley and Pegg 1991).

Decarboxylase activity is reported to be stimulated by putrescine for *T. cruzi* and human enzymes but not plant (Stanley and Pegg 1991; Kinch, Scott et al. 1999; Park and Cho 1999). For *T. cruzi* AdoMetDC, putrescine reduces k_{cat} , while in the human enzyme putrescine exerts its effects on K_{m} . For the human enzyme, residues E11, K80, E178 and E256 are important for putrescine stimulation of activity (Stanley and Pegg 1991). Residues critical for putrescine

stimulation of *T. cruzi* AdoMetDC activity will be discussed later in this work (Clyne, Kinch et al. 2002).

3. Enzyme structure

Unfortunately, the *T. cruzi* AdoMetDC structure has not been solved; however, structures of human and potato AdoMetDCs have (Ekstrom, Mathews et al. 1999; Ekstrom, Tolbert et al. 2001; Tolbert, Ekstrom et al. 2001; Bennett, Ekstrom et al. 2002; Tolbert, Zhang et al. 2003; Toms, Kinsland et al. 2004). The human structure has been solved both with and without inhibitors and as mutant structures that have trapped the enzyme in its pre-processed form. Putrescine is bound in all of the human structures; no putrescine is found in the potato enzyme.

Both human and potato structures reveal a novel fold for AdoMetDC, even when compared with other pyruvoyl-dependent decarboxylases (Ekstrom, Mathews et al. 1999). The human enzyme is a dimer while the potato enzyme is a monomer. Each monomer of AdoMetDC consists of a 4 layer α/β sandwich made of 2 anti-parallel 8 stranded β sheets flanked by several α and 3_{10} helices. The internal symmetry suggests an ancient gene duplication.

The human AdoMetDC structures with bound inhibitors reveal important residues for inhibitor and substrate contacts (Figure 1.5) (Tolbert, Ekstrom et al. 2001). F7 and F223 are important for ring-stacking interactions with the substrate-analog inhibitors MAOEA and MHZPA. Mutation of these residues greatly decreases activity, but it also decreases inhibition. E247 and the mainchain carboxyl of L65 H bond with a hydroxyl on the ribose ring, and T245 indirectly H bonds the inhibitor through a water molecule. Also, the adenosine moiety is bound in the unusual syn conformation.

The putrescine binding site in the human enzyme is buried between 2 β sheets and consists of several charged residues, a unique quality in the interior of

a protein (Figure 1.5) (Ekstrom, Tolbert et al. 2001). Putrescine hydrogen bonds directly to E15, T176 and D174 and indirectly through water to E15, E178, E256 and S113 (Figure 1.5). The carbon chain of putrescine makes favorable hydrophobic interactions with F111, F285 and Y318. The analogous site in the plant enzyme also contains charged residues, with 4 important substitutions: R13, R111, V174 and H285 (Figure 1.4) (Bennett, Ekstrom et al. 2002). The position of the sidechains of the two Arg residues is very similar to the position of the 2 positively charged amines of the putrescine molecule in the human structure. Additionally, H285 is close to that position and could also be positively charged. The negatively charged residues that make contacts with putrescine in the human site are relatively conserved in the potato enzyme. So, the hydrogen bonding network connecting the putrescine site to the active site is preserved. This not only explains why putrescine does not bind the plant enzyme but also why the enzyme is fully active in the absence of putrescine.

Although there is no structure for *T. cruzi* AdoMetDC, sequence alignments can be used and superimposed onto the human and potato structures (Figure 1.4). The *T. cruzi* putrescine binding site appears to have elements of the potato and human enzymes, as well as its own little twist. Position 13 is an Arg, like plant, while positions F285 and D174 are similar to human. S111, I80, and S178 are important divergences from both human and potato enzymes. The position of the putrescine binding site in *T. cruzi* is likely slightly different and more exterior on the protein than the human enzyme. This is supported by differences at positions 13 and 111. R13, which is L in the human enzyme, is similar to plant, and the position of this sidechain interferes with the position of the putrescine in the human structure, both sterically and electrostatically. Also, S111 is not capable of making the same favorable hydrophobic interactions with the putrescine carbon chain as the Phe in the human sequence. The preservation of a negative charge at D174 would still allow the putrescine to bind in this

vicinity, however. Mutational analysis at these positions in the *T. cruzi* enzyme will shed light on the position of the putrescine binding site and will be one of the topics covered in this dissertation.

4. AdoMetDC inhibitor studies

As mentioned earlier, AdoMetDC is a potential drug target because inhibitors of this reaction will prevent spermidine and spermine from being formed. Cell lacking these higher polyamines are incapable of growth and differentiation.

Several substrate/ product analogs have been synthesized in hopes of finding novel inhibitors (Pegg and McCann 1992). Successful inhibitors of this type include S-(5'-deoxy-5'-adenosyl)methylthioethylhydroxylamine (AMA), 5'-deoxy-5''-[(3-hydrazino-propyl)methylamino]adenosine (MHZPA), 5'-deoxy-5'-[(2-aminooxyethyl)-methylamino]adenosine (MAOEA) and 5'-{[(Z)-4-amino-2-butenyl]methylamino}-5'-deoxyadenosine (MDL 73811). AMA and MHZPA covalently bond to the active site pyruvoyl, thus inactivating the enzyme. AMA, MHZPA and MAOEA all work *in vitro* and *in vivo*, but they are not biologically stable enough to develop as drugs. MDL 73811 inactivates the enzyme through transaminating the pyruvoyl to give an alanine. Its rate of inactivation of the human enzyme is stimulated by putrescine. MDL 73811 has been shown to increase AdoMet levels in trypanosomes, but not in humans. MDL 73811 enters trypanosomes through the polyamine transporter but does not enter human cells in the same manner. These species specific differences further the idea that an effective, selective AdoMetDC inhibitor can be made against trypanosomes.

One of the first known inhibitors of AdoMetDC was methylglyoxal bis(guanyl)hydrazone (MGBG) (Figure 1.6). It is a competitive inhibitor that exhibits strong antineoplastic activity. However, MGBG is very non-specific,

inhibiting multiple cellular targets, and has toxic effects, rendering it unacceptable as a curative agent (Pegg and McCann 1992).

Several MGBG analogs have been synthesized and their inhibition of AdoMetDC assessed. Two of these analogs, CGP 40215 and CGP 48664, have been studied as anti-cancer, anti-filarial and anti-trypanosomal agents (Figure 1.6). CGP 40215 has an IC_{50} of 0.0045-0.78 μ M for varying stocks of *T. brucei rhodesiense* while exhibiting an IC_{50} of 1.14mM for human HT-29 cells (Brun, Buhler et al. 1996). This disparity in IC_{50} is most likely due to P2, a unique adenosine transporter in trypanosomes. It has been shown that the mammalian adenosine transporter does not take up MGBG analogs, but P2 does (Tye, Kasinathan et al. 1998). This is another level at which drug selectivity is possible. *In vivo*, mice infected with *T. brucei brucei* who were given 10mg CGP 40215/kg/day for 3 days were all cured (Bacchi, Brun et al. 1996). CGP 40215 was shown to inhibit the AdoMetDC from *Onchocerca volvulus* with a K_i of 5nM (Da'dara, Mett et al. 1998). Also, CGP 40215 was capable of curing *T. brucei rhodesiense* infections in African green monkeys when given at doses of 4mg/kg intramuscularly for 1 week (Brun, Burri et al. 2001). Unfortunately, curative levels of the drug were not found in cerebrospinal fluid, so CGP 40215 would not be able to cure 2nd stage infections. CGP 48664 has an IC_{50} of 0.49-4.46 μ M for various stocks of *T. brucei rhodesiense* while its IC_{50} against the human cell line HT-29 was only 15.5mM (Brun, Buhler et al. 1996). *In vivo*, CGP 48664 was capable of curing murine *T.b. rhodesiense* infections when given at 50mg/kg/day intraperitoneally, 3 times a day for 3 days (Bacchi, Brun et al. 1996). Finally, CGP 48664 has been shown to decrease growth in breast cancer cells (Thomas, Shah et al. 1999). The mechanism of CGP 48664 inhibition of cell growth was studied in the mouse leukemia cell line L1210 (Svensson, Mett et al. 1997). The CGP 48664 IC_{50} for L1210 cells is 100nM (Dorhout, Odink et al. 1997). 2 μ M CGP 48664 was shown to deplete spermidine and spermine levels while greatly

increasing putrescine levels (Svensson, Mett et al. 1997). It caused an increase in the translation of AdoMetDC, but not in its transcription. CGP 48664 does not enter cells through the polyamine transporter. It is also capable of stabilizing the enzyme against degradation. This last point is likely important because AdoMetDC has a rapid turn over rate in the cell. The effect of CGP 40215 and CGP 48664 on *T. cruzi* AdoMetDC, as well as residues important for drug action, will be discussed in this work.

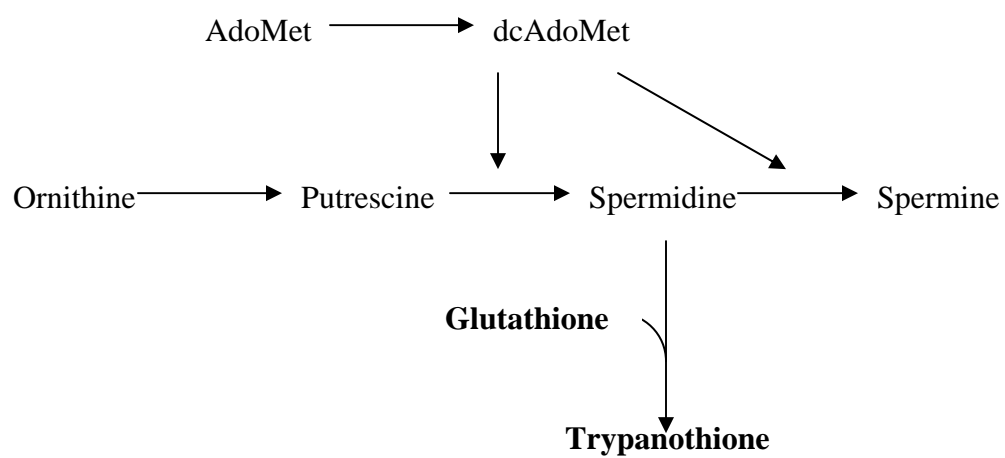


Figure 1.1 Polyamine biosynthetic pathway. Bold items are unique to trypanosomes.

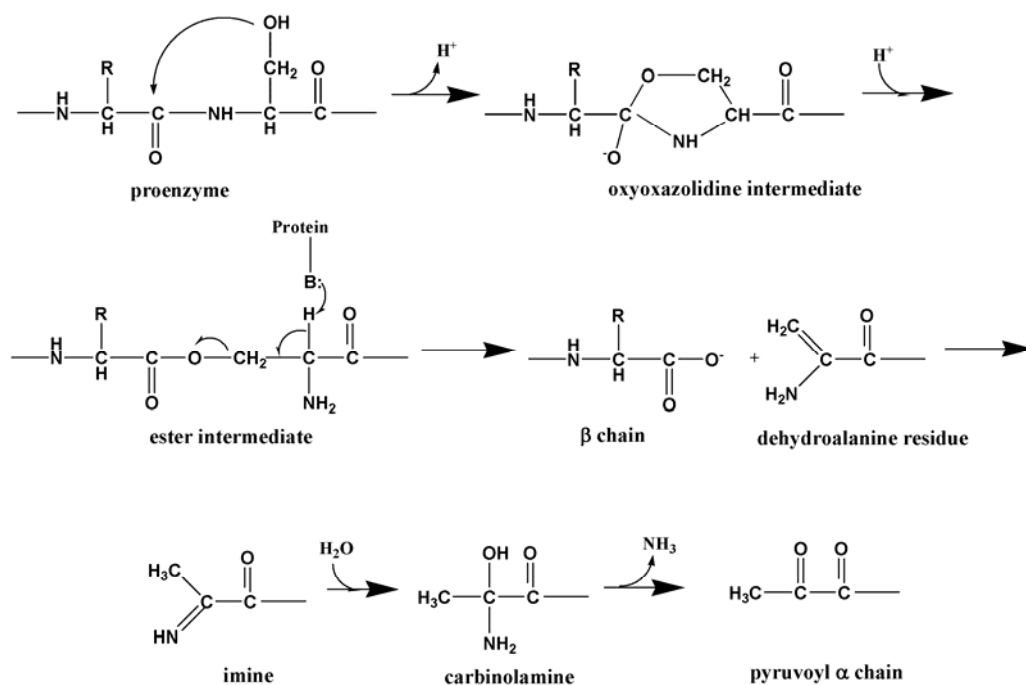


Figure 1.2 Proposed processing reaction mechanism for AdoMetDC (Ekstrom, Tolbert et al. 2001)

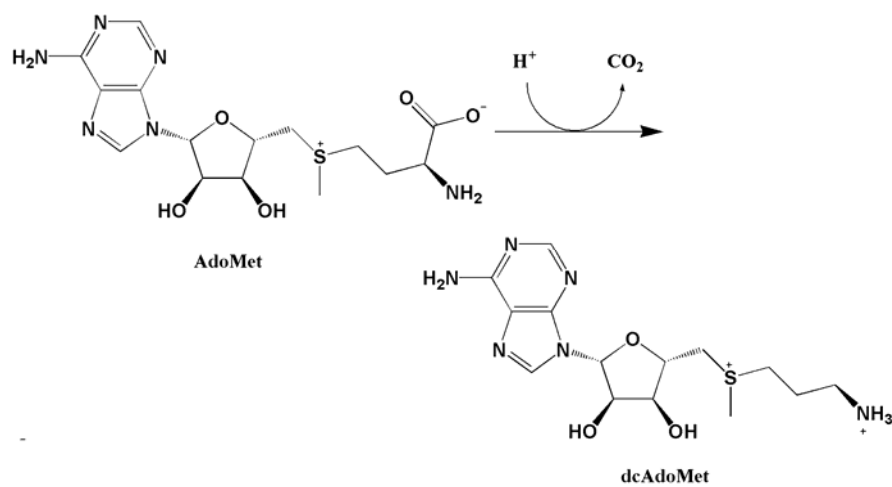


Figure 1.3 Decarboxylation of AdoMet

```

1  MLNKPDLPLSLMAMWGSVKGYDPNQGASFEGPEKRLEIVIMRIT...DETHSEGLHALGDGVWKGVVGSLNAQIVSKESNEY cru
1  .....MEMDLPVSAIGFEGPEKRLEISFVEPGLFADPNGKGLRSLSKAQLDEILGPAECTIVDNLSNDY pot
1  .....MEAAHFEGTEKLELVWFSRQQPDANQSGDLRTIPRSEWDILLKDVQCSIISVTKTDK hum
      *
78  IRSYVLTESSLFVMRDRIILITTCGTTTLNNAVPFVLDVAVSDVRG...EVEWVSFMHKNSFPWEQKGPHLSMAEEFNTLRT cru
65  VDSYVLSESSLFVYSYKIIIKTCGTTLLLAIPPIRLAETLSL...KVQDVRYTRGSFIFPGAQSFPHRHFSEEAVLDG pot
60  QEAYVLSESSMFVSKRRFILKTCGTTLLKALVPLLKLARDYSGFDSIQSFFYSRKNFMKPSHQGYPHRNFQEEEIEFLNA hum

156 YFP...SGKPFIFGPVDS.DHYFLFVYDDVIRPCETENDTQLSMTMYGLDRTQTKHWFSDRFISTGTETAAIRKATKLN cru
143 YFGKLAAGSKAVIMGSPDKTQKWHVYSASAGP.VQSNDPVYTLEMCMTGLDREKASVFYKTEESS...AAHMTVRSGIR pot
140 IFP...NGAGYCMGRMNS.DCWLYLTLDFFESRVISQPDQLEILMSELDPAVMDQFYMKGVT...AKDVTRESGIR hum

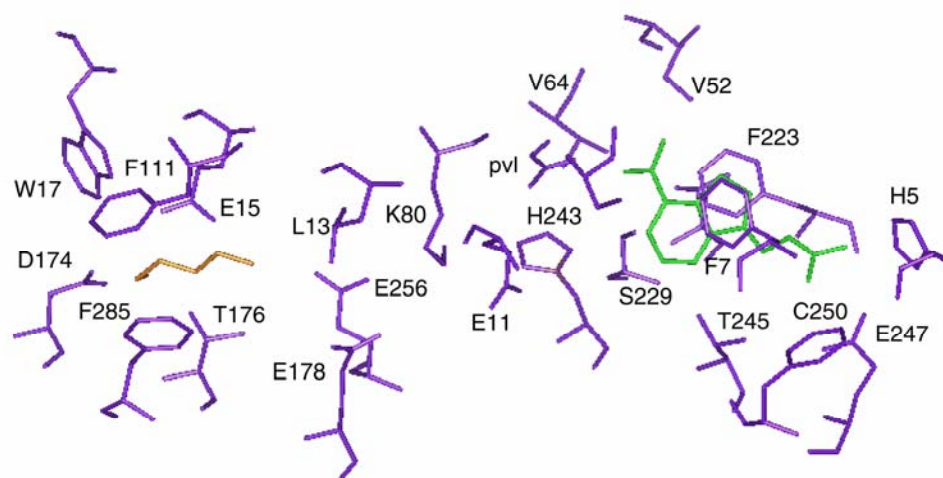
231 KVADDSWKLHDLQFEPCGYSINTIR.GAEYQTIHITPEDHCSFASYET...NTPAVNYSERINTVLGVFAPIRFSVIVFI cru
218 KILPKSEIC.DFEFEPCGYSMNSIEGAAV.STIHITPEDGFSYASFESVGYNPKTMELGPLVERVLACFEPAEFSIALHA pot
211 DLIPGSVI.DATMFNPCGYSMNGMKSDGTYWTIHITPEPEFSYVSFET...NLSQTSYDDLIRKVVEVFKPGKFVTTL... hum

307 DPDS.D.VGRLYQKGQNVGVEAEYYPKYELQNRTVNEFAPGVVVMKMNYARRAEVAEKDSTDSVEE cru
296 DVATKLLERTCSVDVKGYSLAEWSPEEFGEGSIVYQKFTTPYCESPKSVLKGCWKEEKEGKE pot
285 .....FVNQSSKRTVLASPQKIEGFKRLDCSAMFNDYNFVTSFAKKQQQQS..... hum

```

Figure 1.4 AdoMetDC sequence alignment for *T. cruzi*, potato and human enzymes, prepared using clustalw (www2.ebi.ac.uk/clustalw). Fully conserved residues are in bold. The asterisk marks the processing site.

A



B.

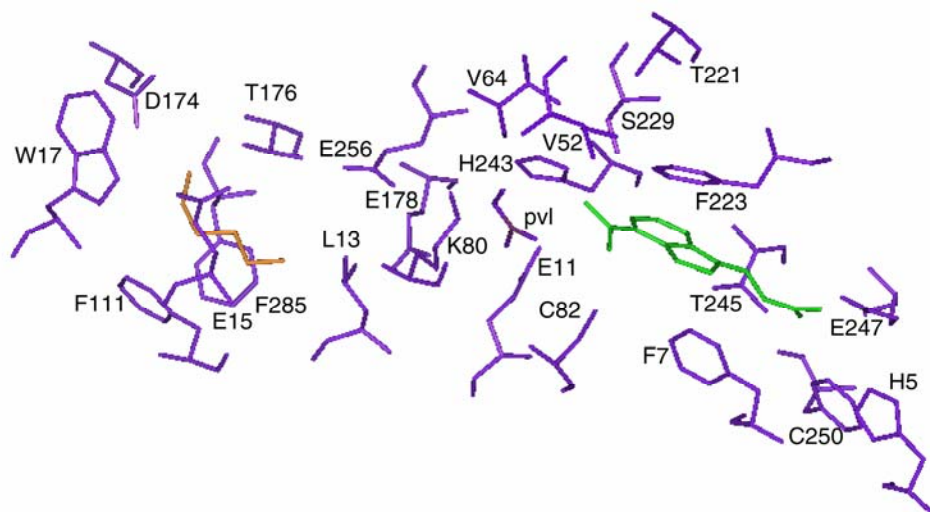


Figure 1.5 Structure of the putrescine and active sites of human AdoMetDC. Panel A is a clear view of the putrescine site and panel B is a clear view of the active site. AdoMetDC is shown in purple, putrescine is shown in orange, and CGP 48664 is shown in green. Pvl is the pyruvate cofactor. The figure was created from PDB file 1I7M using Insight II.

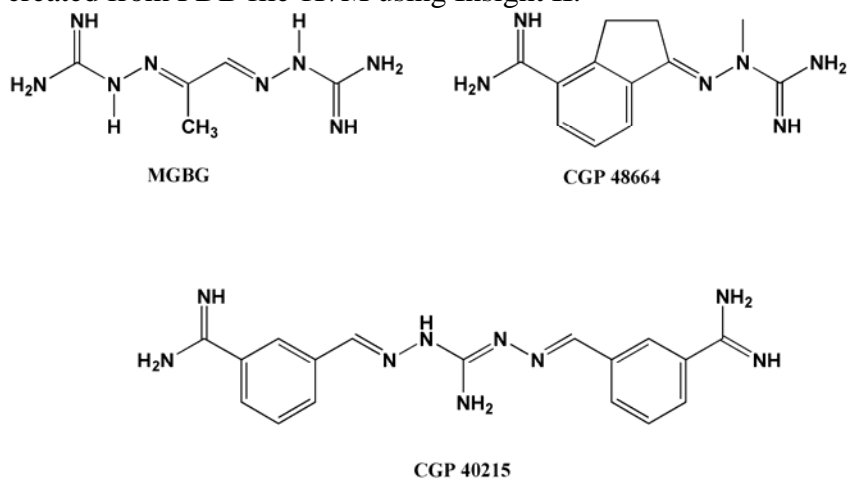


Figure 1.6 Structures of AdoMetDC inhibitors

	$k_{\text{cat}}, \text{s}^{-1}$	$K_{\text{m}}, \mu\text{M}$
<i>T. cruzi</i>	0.06	100
Human	0.5	78
<i>S. cerevisiae</i>	0.9	90
plant (various species)	3-46	8-40

Table 1.1 Kinetic parameters for various AdoMetDCs in the presence of putrescine.

Chapter 2

Mechanism of putrescine stimulation of *T. cruzi* AdoMetDC

A. Introduction

Processing and decarboxylation of human AdometDC are stimulated by putrescine, while plant enzymes are unaffected by the polyamine. It had been shown previously that the decarboxylase activity of *T. cruzi* AdoMetDC is stimulated by putrescine (Kinch, Scott et al. 1999). However, putrescine's role in processing and the mode by which it stimulates decarboxylase activity had not been determined for *T. cruzi*. To gain insight into the structural basis for the effect of putrescine on these processes, mutant enzymes were created based on residues known to be important for human putrescine stimulation (Table 2.1). Additionally, we made mutation R13L based on a sequence alignment of human, potato and *T. cruzi* AdoMetDCs. Buried in the proposed putrescine site of the human enzyme, Position 13 is conserved as a Leu among mammalian enzymes, but is conserved as an Arg in trypanosomal and plant enzymes (Table 2.1, Figure 2.1). Our hypothesis was that this position could account for some of the differences seen in putrescine activation of the 3 enzymes.

To measure putrescine's effect on processing, in vitro transcription/translation reactions were undertaken in the presence and absence of putrescine. Processing of the wild type *T. cruzi* enzyme is unaffected by putrescine. The R13L mutant of *T. cruzi* AdoMetDC is unable to process and processing is not rescued by addition of putrescine. These data suggest that the amino acid substitution at this position is an important structural change that removes a role for putrescine in the processing reaction of the parasite enzyme.

The method by which putrescine activates enzyme activity in the *T. cruzi* enzyme was also studied. One way putrescine could act is by influencing oligomerization. Human AdoMetDC is a dimer, but its interface is not required to form the active site. However, dimerization could allosterically link the two active sites and have an effect on decarboxylase activity. The oligomerization state for *T. cruzi* AdoMetDC was previously unknown. I used analytical ultracentrifugation to determine the oligomerization state in the presence and absence of putrescine. Another way putrescine could enhance catalytic activity is by forming a Schiff base with the pyruvate cofactor. To test this, we attempted to reduce ^{14}C -labeled putrescine onto enzyme. However, no putrescine was covalently linked to the enzyme after reduction. The last possibility for putrescine's mode of stimulation is that of binding to an activator site. To examine putrescine binding, an intrinsic fluorescence assay was used. This showed that putrescine is bound more weakly to the *T. cruzi* enzyme than to the human enzyme. Of the residues that are important for putrescine activation of human AdoMetDC, only D174 plays a role in putrescine binding and stimulation of the *T. cruzi* enzyme. These studies demonstrate that putrescine plays different roles in the function of AdoMetDC from different organisms, and that it is likely to have a different binding mode in the parasite enzyme.

B. Experimental Procedures

1. Materials

S-Adenosyl[*carboxy*- ^{14}C]methionine (56 mCi/mmol) and [^{14}C]putrescine (114 mCi/mmol) were purchased from Amersham Pharmacia Biotech (Arlington Heights, IL). Ni^{2+} -agarose was purchased from Qiagen Inc. (Chatsworth, CA). Restriction enzymes were purchased from New England Biolabs (Beverly, MA)

or Boehringer Mannheim (Indianapolis, IN). All other reagents were purchased from Sigma (St. Louis, MO).

2. Expression and Purification of *T. cruzi* AdoMetDC

AdoMetDC was expressed and purified as a His-tagged fusion using the gene cloned from *T. cruzi* in a T7 bacterial expression construct as previously described (Kinch, Scott et al. 1999). *Escherichia coli* BL21/DE3 cells containing this construct were grown in a New Brunswick BioFlo 3000 fermentor, and the recombinant enzyme was purified using Ni²⁺-agarose column chromatography and anion exchange column chromatography. All purification buffers lacked putrescine. The purified protein was quantitated using the extinction coefficient previously determined for the native enzyme (46.5 mM⁻¹ cm⁻¹).

3. Human AdoMetDC Cloning and Expression

The human AdoMetDC gene was amplified from human prostate QUICK-Clone™ cDNA (Clontech Labs, Inc.) using the PCR primers 5'-TGGGCCCCATGGAAGCTGCACATTTTTTCGAAGGGACCG-3' and 5'-ACGCTGTCTGACTCAACTCTGCTGTTGTTGCTGCTTCTTAGC-3'. The PCR product was cloned into the *Nco*I and *Sal*I sites of the expression plasmid ODC29 (Osterman, Grishin et al. 1994) to generate the human expression plasmid pSam18. The human insert was sequenced, and the protein was expressed and purified as previously described for the *T. cruzi* enzyme (Kinch, Scott et al. 1999). The resulting clone contains a single mutation (R33C) that we found fortuitously increases the expression levels without affecting function. This residue is not fully conserved across different species and is located on the surface of the enzyme distant from the active site and the putative putrescine binding site. The human enzyme expresses to high levels, producing 200 mg of purified enzyme from a 6 L preparation. The purified recombinant protein is correctly processed

into a 31 kDa α subunit and a 7.5 kDa β subunit. Gel filtration of the recombinant human enzyme predicts a molecular mass of 73 kDa in the presence of putrescine, which is consistent with a dimer of $\alpha\beta$ subunits.

4. Site-Directed Mutagenesis of *T. cruzi* AdoMetDC

To create the various mutant AdoMetDC enzymes, PCR-based site-directed mutagenesis using the Stratagene QuikChange kit was performed using the *T. cruzi* AdoMetDC expression plasmid as a template. The constructs were verified by sequencing.

5. *In Vitro* Translation and Proenzyme Processing

Wild-type and mutant AdoMetDC proteins were synthesized *in vitro* using the T7-coupled transcription/translation kit (Promega) with [³⁵S]methionine to label the protein as described previously (Stanley and Pegg 1991). Each reaction included 0.2 μ g of plasmid, 9.4 pmol of [³⁵S]methionine (total volume of 0.05 mL), and 2 mM putrescine when indicated. The transcription/translation reaction mixture was incubated at 30°C for 30 min, at which time cycloheximide was added to a final concentration of 0.2 mM to stop translation. The reaction mixtures were incubated at 30°C to allow proenzyme processing to continue, and aliquots were removed at 0, 15, 30, and 60 min for analysis by a 15% SDS-PAGE. The gel was prepared for autoradiography by fixing in destain (5% MeOH and 7% acetic acid) for 30 min, washing with H₂O, soaking in sodium salicylate for 5 min, and washing with H₂O. The gel was then dried and exposed to Reflection NEF-496 film (Du Pont) overnight. Relative amounts of processed versus unprocessed protein were quantified using NIH image (National Institutes of Health, Bethesda, MD).

6. Analytical Ultracentrifugation

Equilibrium sedimentation data for the *T. cruzi* AdoMetDC enzyme were collected in a Beckman XLI analytical ultracentrifuge. Samples were analyzed at 20°C in buffer [50 mM Hepes (pH 8.0), 100 mM NaCl, and 0.5 mM β -mercaptoethanol] with or without 10 mM putrescine. Three enzyme concentrations (initial absorbances of 0.2, 0.4, and 0.5, respectively) were loaded into a six-sector equilibrium centerpiece and equilibrated at three rotor speeds (11,000, 13,000, and 15,000 rpm). Absorption data were collected through quartz window assemblies at 280 nm, using a radial step size of 0.001 cm, and recorded as the average of 15 measurements at each radial position once samples were judged to have reached equilibrium. The nine data sets for each enzyme were analyzed with Beckman XL-A.XL-I Data Analysis Software version 4.0 and globally fit to the appropriate model using a monomer molecular weight of 43,974 and a molar extinction coefficient of $46\,500\text{ cm}^{-1}\text{ M}^{-1}$. The baseline values were allowed to float, and \bar{v} (0.731 mL/g) and ρ (1.00 g/mL) were fixed during the fit to values determined using the program SEDNTERP (Laue 1992). The goodness of fit was determined by examination of the residuals and minimization of the variance. The data were best fit to a monomer-dimer equilibrium in all cases.

7. Cyanoborohydride Reduction of the Substrate and Activator

To determine the extent of Schiff base formation on the enzyme, sodium cyanoborohydride (NaCNBH_3) was used as a reducing agent (Borch 1971). The reaction mixtures contained wild-type AdoMetDC (430 μM) and either $^{14}\text{CO}_2$ -AdoMet (56 mCi/mol, 44 μM) or $[1,4\text{-}^{14}\text{C}]$ putrescine (114 mCi/mmol, 44 μM) in buffer [200 mM HEPES (pH 7.5)] in a final volume of 0.02 mL. NaCNBH_3 was added to a final concentration of 5 mM, and the reaction mixtures were incubated for 20 min at 37°C and then stored at 4°C overnight. The protein was precipitated by adding 7.5% TCA. The amount of radioactivity was measured in both the

precipitate and the supernatant to determine the extent of Schiff base formation. The precipitated protein was run on SDS-PAGE and stained with Coomassie blue. The extent of radioactive incorporation was visualized after using the EN³HANCE autoradiography enhancer as recommended by the manufacturer (NEN Research Products) with a 6 day exposure.

8. Putrescine Binding Assays

Putrescine Binding As Assessed by Tryptophan Fluorescence. Mixtures of AdoMetDC (1-5 μ M) in buffer [50 mM HEPES (pH 8.0), 50 mM NaCl, and 2.5 mM DTT] were titrated with increasing amounts of either putrescine or NaCl in a total of 1 mL. A difference emission spectrum in the presence and absence of putrescine was generated using a fluorometer (Photon Technology International) to find the wavelength with the largest change upon excitation at 280 nm. The emission spectrum was collected in 1 or 2 nm intervals from 300 to 400 nm in the absence or presence of 10 mM putrescine. The fluorescence intensity in the presence of saturating putrescine (F) was then subtracted from the fluorescence intensity in the absence of putrescine (F_0). Titrations of putrescine were then performed by adding increasing amounts of putrescine (0.02-10 mM) and measuring the emission at 340 nm at 1 s intervals for 20 s. The measurements were repeated, and the 40 fluorescent intensity points were averaged to obtain a single intensity for the putrescine concentration. Under these conditions, very little photobleaching of the enzyme was detected. As a control, increasing amounts of NaCl were added to an equivalent mixture in parallel. The average of the putrescine intensity (F) was subtracted from the average of the NaCl intensity (F_0) and then plotted against putrescine concentration. The K_d for putrescine was then determined by fitting the data to eq 1

$$F - F_0 = \frac{[L]F_{\max}}{K_D + [L]} \quad (1)$$

where L represents the putrescine ligand.

Binding of [¹⁴C]Putrescine. Equilibrium product binding to *T. cruzi* or human AdoMetDC was assessed using ultrafiltration to separate free ligand (Sophianopoulos, Durham et al. 1978). Various concentrations of [1,4-¹⁴C]putrescine (10-320 μ M for *T. cruzi* or 1.5-80 μ M for human AdoMetDC) were mixed with AdoMetDC (80-100 μ M for *T. cruzi* or 9.4 μ M for human AdoMetDC) in buffer [50 mM HEPES (pH 8.0), 50 mM NaCl, and 2 mM DTT]. Mixtures were incubated at 4°C overnight. A microcon-10 microconcentrator (Amicon) was used to separate a small portion of free ligand (5-6 μ L) from the total volume (0.1 mL) by spinning at 14000g for 7 s. The concentrations of free ligand ($[L_f]$) and total ligand were determined by measuring the amount of radioactivity in an aliquot of sample (2 μ L). The bound ligand ($[L_B]$) concentration was calculated by subtracting free from total, and the data were fitted to eq 2.

$$[L_B] = \frac{n[E][L_f]}{K_D + [L_f]} \quad (2)$$

9. Steady-State Kinetic Analysis

Steady-state kinetic analysis of AdoMetDC was performed as previously described (Kinch, Scott et al. 1999). Reactions were carried out in buffer [200 mM HEPES (pH 8.0), 100 mM NaCl, and 5 mM DTT] at various AdoMet (0.01-10 mM) and putrescine concentrations (0-45 mM). Reaction mixtures were incubated at 37°C for 5, 10, and 20 min at various enzyme concentrations (0.5-6.5 μ M) to ensure a linear rate with time. Data were fitted to the Michaelis-Menten equation to determine the rate constants K_m and k_{cat} .

C. Results

1. Effects of Putrescine on Autocatalytic Processing of *T. cruzi*

AdoMetDC. To test if proenzyme processing of *T. cruzi* AdoMetDC is stimulated by putrescine, the enzyme was expressed in an *in vitro* rabbit reticulocyte system in the presence and absence of putrescine. The processing reaction was monitored by SDS-PAGE analysis after addition of cycloheximide and incubation of the translation product for increasing amounts of time. The rate of processing of *T. cruzi* AdoMetDC was not affected by the addition of putrescine (2 mM) to the reaction mixture (Figure 2.2). In contrast, as reported previously (Stanley and Pegg 1991), both the rate and extent of the processing reaction for the human enzyme were increased by the addition of putrescine.

The X-ray structure of human AdoMetDC bound to putrescine identifies the amino acid residues in the binding site (Ekstrom, Tolbert et al. 2001). Several of these residues differ in the *T. cruzi* enzyme, suggesting that the roles and function of putrescine and its interacting residues may also differ. Notably, the *T. cruzi* enzyme contains a positive charge at position 13 (Figure 2.1 and Table 2.1), which is present in the protozoal (including the kinetoplastids and *Plasmodium* species) and plant enzymes. The equivalent residue in the human enzyme is L13, which is 3.4 Å from the bound putrescine residue. To test if the Arg in this position of the *T. cruzi* enzyme is able to substitute for the role of putrescine in the processing reaction, R13 in the *T. cruzi* enzyme was mutated to Leu. The R13L mutant enzyme is expressed as a proenzyme in the rabbit reticulocyte system, but it fails to process to the mature form after extended incubation in the presence or absence of putrescine (Figure 2.2). These data demonstrate that R13 is an essential residue for proenzyme processing in the *T. cruzi* enzyme, and they identify a fundamental difference in the structural requirements for proenzyme activation between the *T. cruzi* and human enzymes.

2. Analysis of Schiff Base Intermediates Formed with *T. cruzi* AdoMetDC by Trapping with Cyanoborohydride.

The putrescine activator contains two free amino groups that could form a Schiff base with the pyruvate cofactor on the AdoMetDC enzyme. Therefore, putrescine could enhance the rate of Schiff base formation with AdoMetDC by allowing the chemistry to proceed through a gemdiamine intermediate instead of a carbinolamine intermediate. Pyridoxal phosphate (PLP)-dependent enzymes utilize this approach to accelerate Schiff base formation with the substrate through the formation of an internal aldimine between PLP and an active site Lys residue (Toney and Kirsch 1989; Toney and Kirsch 1993; Osterman, Brooks et al. 1999). To test this hypothesis, either radiolabeled putrescine or AdoMet was incubated with the *T. cruzi* AdoMetDC enzyme (0.43 mM) and the mixture was treated with sodium cyanoborohydride to reduce any Schiff base species that was formed. The protein samples were evaluated by SDS-PAGE and autoradiography. Radiolabeled AdoMet was readily incorporated onto the protein; however, no radioactive putrescine was detected in the protein band (Figure 2.3). The absence of any radioactivity suggests that the putrescine does not form a Schiff base with pyruvate.

3. Analysis of the Oligomeric State of *T. cruzi* AdoMetDC by Equilibrium Sedimentation.

AdoMetDC is a homodimer of $\alpha\beta$ subunits. The X-ray structure of the human enzyme demonstrates that the active sites are contained within each enzyme monomer and that they are distant from the dimer interface, suggesting that the enzyme is not an obligate dimer (Ekstrom, Mathews et al. 1999). Therefore, an allosteric mechanism would be required for dimerization to influence the decarboxylation rate of the enzyme. To test the hypothesis that putrescine increases AdoMetDC activity by altering the dimeric state of the

enzyme, purified recombinant *T. cruzi* AdoMetDC was analyzed by equilibrium sedimentation in a Beckman analytical ultracentrifuge in the presence and absence of putrescine (10 mM). For each analysis, nine data sets consisting of three different speeds and three different enzyme concentrations were utilized in a global fit of the data to various oligomeric models. In all cases, the data for *T. cruzi* AdoMetDC were best fit by a dimer-monomer equilibrium with a K_d of 15-30 μ M in the absence or presence of putrescine (Figure 2.4). These data demonstrate that the dimer is not essential to the catalytic activity of the protein, as the enzyme is fully active at enzyme concentrations of $<0.5 \mu$ M. Further, putrescine has no effect on the oligomeric state of the enzyme.

4. Assessment of Putrescine Binding to *T. cruzi* AdoMetDC by Fluorescence and by Ultrafiltration.

Intrinsic tryptophan fluorescence measurements provide a method of evaluating ligand interactions in cases where the environment of a Trp residue changes upon ligand binding (Lakowicz 1983). Therefore, the effect of putrescine on the intrinsic Trp fluorescence of the AdoMetDC enzyme was measured. Figure 2.5A illustrates the fluorescence emission spectrum of the *T. cruzi* AdoMetDC enzyme compared to that of free Trp in buffer. The emission maximum (λ_{max}) of the enzyme is shifted toward a wavelength (335 nm) lower than that of the free Trp (355 nm). Because the emission spectrum of Trp shifts to shorter wavelengths as the polarity of the solvent decreases (Freifelder 1982), the measured fluorescence emission of the AdoMetDC enzyme is due to a buried Trp residue on the protein. The addition of putrescine (10 mM) to the enzyme yields a measurable decrease in emission intensity (Figure 2.5B,C), which is accompanied by a slight shift in the peak maximum toward a lower wavelength ($\lambda_{max} = 332$ nm). The wavelength showing the maximum difference in the presence of saturating putrescine (340 nm) was then used to further characterize the effects of

putrescine concentration on fluorescence (Figure 2.5D). The data were fitted to eq 1 to determine the dissociation constant (K_d) for the putrescine ligand ($150 \pm 20 \mu\text{M}$).

To provide additional support for the idea that the K_d determined from the fluorescence analysis represents ligand binding, equilibrium binding analysis of radioactive putrescine ($[^{14}\text{C}]$ putrescine) to the *T. cruzi* AdoMetDC enzyme was performed by ultrafiltration (Figure 2.6). The dissociation constant measured by this method ($K_d = 180 \pm 100 \mu\text{M}$, $n = 1.6 \pm 1.1$) is similar to that determined from the fluorescence binding assay. These results validate the use of the fluorescence assay in assessing putrescine binding. Finally, the K_d measured for putrescine binding is significantly lower than the concentration of putrescine ($K_{m,\text{put}} = 4.7 \text{ mM}$) required to fully activate the enzyme (Table 2), reflecting a complexity in the kinetic model of activation.

5. Putrescine Binding to Human AdoMetDC.

Steady-state kinetic analysis of the human AdoMetDC enzyme at pH 8.0 in the presence of the saturating putrescine activator (2 mM) produces a K_m for AdoMet ($70 \pm 17 \mu\text{M}$) and a k_{cat} ($0.7 \pm 0.07 \text{ s}^{-1}$) similar to those previously described (Stanley, Shantz et al. 1994). As previously reported, the overall rate of the human reaction is much faster than that of the parasite enzyme (Kinch, Scott et al. 1999). Comparison of the apparent putrescine activation constants for human and *T. cruzi* AdoMetDC determined by kinetic analysis [for human, $K_{m,\text{put}} = 0.13 \text{ mM}$ (Zappia, Carteni-Farina et al. 1972); for *T. cruzi*, $K_{m,\text{put}} = 4.7 \text{ mM}$ (Table 1)] suggests that putrescine may bind tighter to the human AdoMetDC than to the parasite enzyme. However, kinetic analysis does not allow for the measurement of a true dissociation constant. Therefore, binding of putrescine to the human enzyme was also studied by fluorescence and by equilibrium binding to $[^{14}\text{C}]$ putrescine. The human enzyme exhibits a smaller change in the

fluorescence emission intensity in the presence of the putrescine activator than the *T. cruzi* AdoMetDC enzyme, and instead of a decrease in fluorescence being seen, an increase is observed (Figure 2.5E). The maximum fluorescence emission intensity difference occurred at 332 nm, and it varies with putrescine concentration. Titration of the fluorescence emission intensity at 332 nm was used to measure a binding isotherm for putrescine ($K_d = 5 \pm 3 \mu\text{M}$). The K_d determined by fluorescence is again similar to that measured by Scatchard analysis of equilibrium binding of the human AdoMetDC enzyme to [^{14}C]putrescine ($K_d = 6 \pm 1 \mu\text{M}$, $n = 1.5 \pm 0.1$), validating the fluorescence method for the human enzyme. The data demonstrate that the human enzyme binds putrescine with a higher affinity than the parasite enzyme; thus, the differences in putrescine concentration required to activate the two enzymes are also reflected in a difference in affinity. However, as with the *T. cruzi* enzyme, the K_d for putrescine is significantly lower than the $K_{m,\text{put}}$ (0.13 mM) reported for the human enzyme based on kinetic analysis (Zappia, Carteni-Farina et al. 1972). Thus, kinetic analysis of enzyme activation by putrescine does not provide direct information about binding affinity for putrescine in either the *T. cruzi* or the human enzyme.

6. Site-Directed Mutagenesis of Putative Putrescine Binding Site Residues.

A number of residues have been identified in the putrescine binding site of human AdoMetDC [E15, K80, D174, E178, and E256(Ekstrom, Tolbert et al. 2001); Figure 2.1], and several of these residues have been reported to be required for putrescine stimulation of activity [D174, E178, and E256(Stanley and Pegg 1991; Xiong, Stanley et al. 1997)]. Of these residues, E15, E256, and D174 are conserved in the *T. cruzi* enzyme while E178 and K80 are not (Table 2.1). To determine the roles of these residues in the putrescine activation of the *T. cruzi*

enzyme, these residues were mutated. The conserved residues E15 and E256 were replaced with Ala, and D174 was mutated to Val, the residue found in this position in plants (Table 2.1). E178 and K80 form a salt bridge in the human enzyme. These residues are neutral residues in the *T. cruzi* enzyme (I80 and S178). The double mutant I80K/S178E was constructed in the *T. cruzi* enzyme to create an enzyme that contained the same residues as the human enzyme in these positions. All four mutant enzymes (E15A, E256A, D174V, and I80K/S178E) were expressed normally and were processed to the mature form of the enzyme.

The effects of the mutations on putrescine binding and activation were characterized for each. E256A and I80K/S178E bind putrescine with an affinity similar to that of the wild-type enzyme, as measured by the fluorescence binding assay, while E15A binds with a 10-fold higher affinity (Table 2.2). I80K/S178E is activated by putrescine to the same extent as wild-type *T. cruzi* AdoMetDC (Table 2.2). However, E15A and E256A were activated to a lesser extent than the wild-type enzyme; the k_{cat}/K_m increased by 2- and 4-fold for E15A and E256A, respectively, in comparison to 11-fold for the wild-type enzyme (Table 2.2). Thus, while these mutations do not disrupt putrescine binding, these residues do play some role in the mechanism of activation.

In contrast to these results, the fluorescence emission spectrum of the D174V mutant enzyme does not change as putrescine is titrated into the enzyme mixture over a broad concentration range of 0.02-10 mM putrescine (Figure 2.5F). Further, the D174V mutant is not activated by putrescine; the k_{cat}/K_m is unchanged in the presence of 45 mM putrescine (Table 2.2). These results demonstrate that the D174V mutant *T. cruzi* enzyme no longer binds putrescine, consistent with a role for D174 in forming a direct interaction with the positive charge of the putrescine. Thus, D174 is the one residue that plays a common role in putrescine binding between the mammalian and parasitic enzymes.

D. Discussion

The role of putrescine in AdoMetDC processing and enzyme activity differs among the enzymes from different species. For the human enzyme, putrescine stimulates both processing and enzyme activity, while for the plant enzymes, putrescine plays no role in either process (Zappia, Carteni-Farina et al. 1972; Poso, Sinervirta et al. 1975; Ekstrom, Tolbert et al. 2001). While putrescine stimulates the activity of the *T. cruzi* enzyme, the data presented herein demonstrate that it has no role in proenzyme processing. Analysis of the amino acid sequences of the AdoMetDC enzymes from these various species provides clues about the involvement of different residues in the binding and activation process, therefore shedding light upon the physical basis of these responses. The residues making up the central core of the putrescine binding site of the human AdoMetDC enzyme contain several significant differences among enzymes from different species (Figure 2.1 and Table 1). Our data suggest that the substitution of an Arg residue for Leu at position 13 eliminates a role for putrescine in the proenzyme processing reaction of the *T. cruzi* enzyme, while the residue at position 174 determines if putrescine stimulates enzyme activity.

The residue at position 13 is Leu in the human enzyme and Arg in the *T. cruzi* and plant enzymes. This residue is within 3.4 Å of the putrescine binding site in the human AdoMetDC structure (Ekstrom, Tolbert et al. 2001). Mutation of R13 to Leu in the *T. cruzi* enzyme renders the enzyme unable to process to the mature form, in either the presence or absence of putrescine. These data suggest that the presence of the positive charge at this position may mimic the positive charge of the putrescine molecule. Thus, this amino acid change is a key structural difference in the parasitic and plant enzymes that may underlie the finding that putrescine no longer plays a role in the proenzyme activation process. The requirement for putrescine in the processing reaction for the human enzyme is not however as strict as the requirement for R13 in the *T. cruzi* enzyme. The

human enzyme is processed in the absence of putrescine, just at a slower rate (Xiong, Stanley et al. 1997). In addition, the processing of the *N. crassa* enzyme, which also has a Leu at position 13, is not stimulated by putrescine (Hoyt, Williams-Abbott et al. 2000). Thus, R13 in the *T. cruzi* enzyme is likely to have additional functional roles in the processing reaction beyond the role of putrescine in the human enzyme, and additional structural differences between the enzymes may also be required to fully manifest these functions.

Insight into the mechanism by which putrescine stimulates enzyme activity in the *T. cruzi* enzyme can also be obtained by comparative analysis. D174 is conserved in the human and *T. cruzi* enzymes but is substituted with a Val in the plant enzymes (Table 2.1). The *T. cruzi* mutant enzyme D174V no longer binds putrescine, nor is it activated by putrescine. A similar result was reported for the activation of the mutant human enzyme D174V, though direct analysis of putrescine binding was not undertaken (Xiong, Stanley et al. 1997). Thus, the plant enzymes that contain Val at position 174 and Arg at position 13 would not be expected to bind putrescine, consistent with the observation that neither processing nor enzyme activity is affected by putrescine. The enzyme from *Plasmodium falciparum* also lacks D174, and consistent with this structural change, the activity of this enzyme is not activated by putrescine.

The fact that putrescine cannot substitute for the absence of the positive charge in the R13L mutant processing reaction suggests that the diamine does not have the same binding mode on the parasite enzyme as observed for the human enzyme. Inspection of the putrescine binding site in the human structure provides additional support for this interpretation (Figure 2.1). The positive charge on R13 would be expected to have an unfavorable electrostatic interaction with putrescine if it were bound in the same site as observed for the human enzyme. In addition, the presence of the larger side chains of R13, Q176, and M113 in the binding site would also provide a likely steric block to ligand binding at this site. The

mutagenesis data on the *T. cruzi* enzyme are consistent with this hypothesis. Mutation of E15 and E256, which are conserved in the putrescine binding site between human and *T. cruzi* AdoMetDC, had no effect on putrescine binding in the *T. cruzi* enzyme. The ion pair of E178 and K80 found in human AdoMetDC is replaced with Ser and Ile in the parasite enzymes. Mutation of these residues in the human enzyme results in an impaired ability of the enzyme to be activated by putrescine (Stanley and Pegg 1991; Stanley, Shantz et al. 1994). In contrast, mutation of the *T. cruzi* residues to the ion pair found in the human enzyme had virtually no effect on putrescine binding or activation. Collectively, the lack of an influence of these residues on putrescine binding and activity suggests that the bound putrescine on the *T. cruzi* enzyme has been displaced from the position that is observed for the human enzyme and that it binds in a site that is at most only partially overlapping.

Although the exact position of the putrescine binding site in *T. cruzi* AdoMetDC awaits structure determination, clues to its position can be inferred from the comparative analysis of mutations described in this paper. D174 is the one common residue that appears to be involved in putrescine binding for both the *T. cruzi* and human enzymes. This residue is the most solvent-exposed of the interacting residues observed in the human enzyme structure. The more interior amino acid residues (E15, E256, K80, and E178) do not play a role in putrescine binding to the parasite enzyme, suggesting the binding site may be located closer to the surface. Further, the 10-fold decrease in putrescine affinity for the parasite enzyme suggests weaker interactions in the binding site that may stem from a more exposed location.

Finally, the observed fluorescence changes upon putrescine binding (Figure 2.5) suggest that the two enzymes exhibit a different environment surrounding the emitting Trp residue or residues. As a number of different Trp residues exist in both the human and *T. cruzi* enzymes, identification of the

residues involved in the fluorescence change is difficult. However, both enzymes contain Trp residues (*T. cruzi* W109 and human W17) in the proximity of the common putrescine binding determinant D174. The carboxylate oxygen of D174 is 4.8 Å from the indole nitrogen of W17, while the side chain of position 109 is 2 Å further from both D174 and N α 1 of putrescine than is position 17 (Figure 2.1). These data are also consistent with a more exterior binding site for putrescine in the *T. cruzi* enzyme. Finally, the substitution of W17 with Ile, and F111 with Ser in the *T. cruzi* enzyme, could provide space for the putrescine binding site to be accommodated in this location.

We have used the differences in the activation of the human and parasite AdoMetDC enzymes to elucidate features of the putrescine binding site on the *T. cruzi* enzyme. Our data suggest that positions 13 and 174 are key determinants in the activation of processing and enzyme activity by putrescine. The parasite enzyme does not require putrescine to activate the processing reaction but instead Arg-13 is a major structural determinant required in the processing reaction. D174 plays a role in binding putrescine in both the human and *T. cruzi* enzymes; however, the putrescine binding site is likely to be only partially overlapping between the two structures.

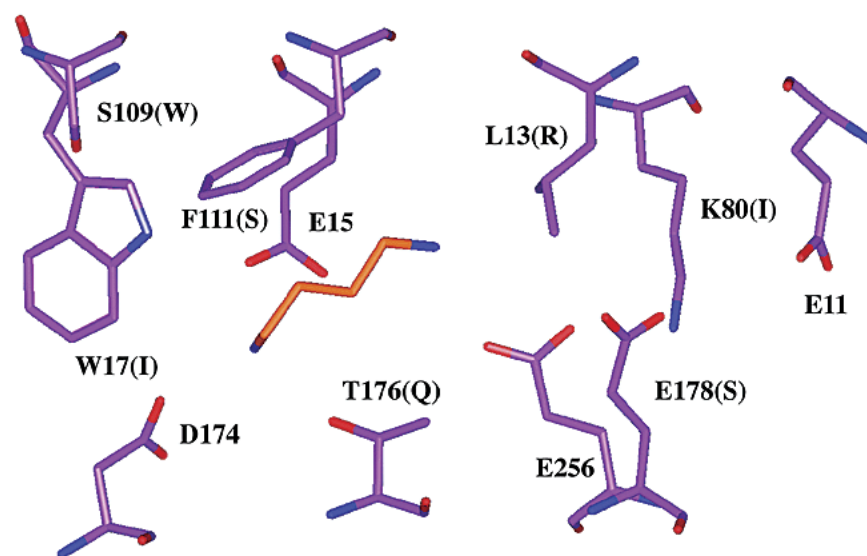


Figure 2.1 Structure of Human AdoMetDC putrescine (orange) binding site.

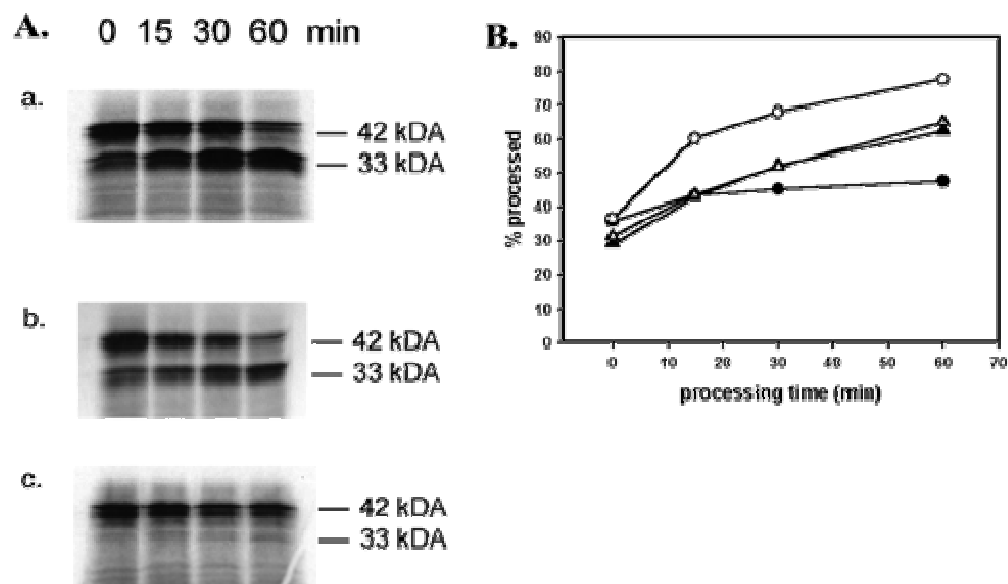


Figure 2.2 Proenzyme processing of *T. cruzi* and human AdoMetDC. (A) *T. cruzi* AdoMetDC was expressed in an *in vitro* rabbit reticulocyte system in the presence of [³⁵S]Met. After 30min, reactions were stopped by the addition of cycloheximide and the mixtures were incubated for 0,15,30, and 60 min before analysis. The protein was subjected to SDS-PAGE and visualized by autoradiography: (a) wild-type in the absence of putrescine, (b) wild-type in the presence of 2mM putrescine and (c) R13L *T. cruzi* AdoMetDC in the presence of 2mM putrescine. (B) Percent of the processed enzyme plotted vs. incubation time: human AdoMetDC (circles) and *T. cruzi* AdoMetDC (triangles), without putrescine (filled) and with putrescine (open).

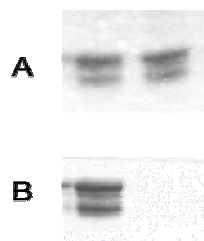


Figure 2.3 Analysis of Schiff base intermediates formed with *T. cruzi* AdoMetDC. [14CH₃]AdoMet (lane 1) and [14C]putrescine (lane 2) were incubated with *T. cruzi* AdoMetDC and reduced with sodium cyanoborohydride. Panel A shows a Coomassie blue-stained SDS gel (15%) of the AdoMetDC α subunit. Panel B shows a 6 day exposure of the same gel and represents the radioactive ligand covalently attached to the α subunit after reduction. The α subunit typically runs as two bands on SDS-PAGE ((Kinch, Scott et al. 1999).

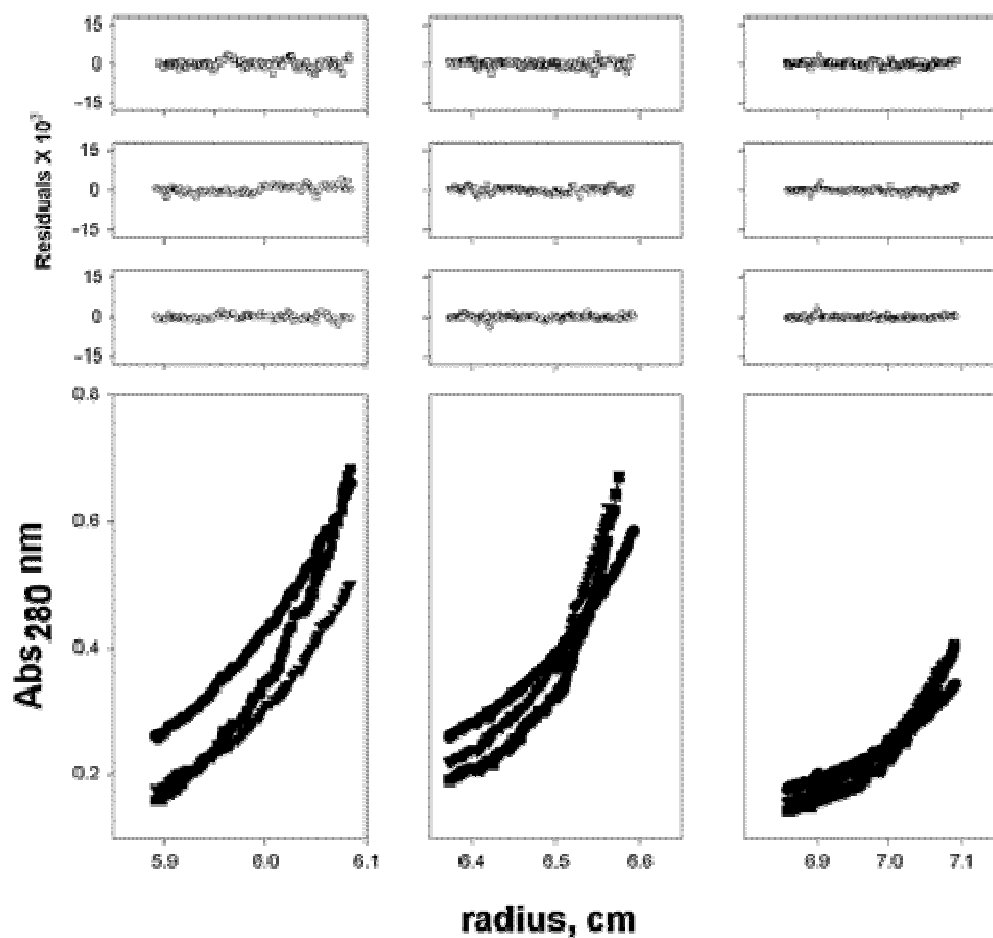


Figure 2.4 Sedimentation equilibrium analysis of *T. cruzi* AdoMetDC. A representative data set in the presence of putrescine is displayed. Dimerization constants (K_d) were determined by global analysis of nine data sets acquired at three speeds and three protein concentrations. For this data set, $K_d = 14\mu\text{M}$ with a 95% confidence limit of 12-16 μM .

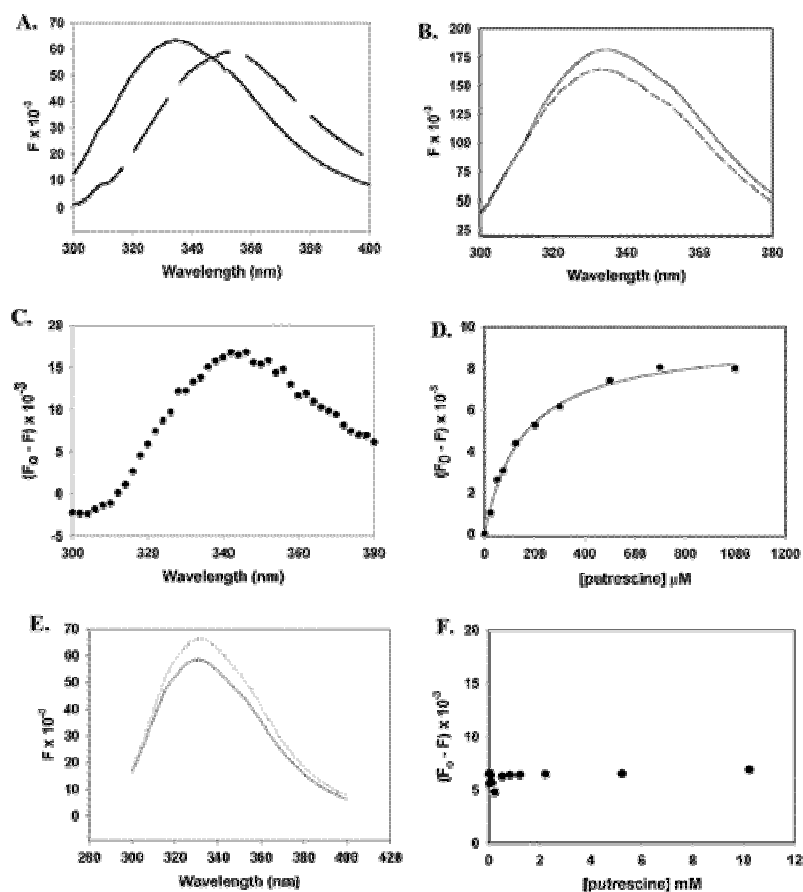


Figure 2.5 Analysis of putrescine binding to *T. cruzi* AdoMetDC by intrinsic fluorescence emission. Panel A shows the fluorescence (F) emission spectrum of *T. cruzi* AdoMetDC (-) and tryptophan (---) after excitation at 280nm. The λ_{\max} for the enzyme is 335 nm, while the λ_{\max} for tryptophan is 335nm. Panel B shows the fluorescence emission change of *T. cruzi* AdoMetDC (-) upon addition of 10mM putrescine (---). Panel C shows the difference spectrum of the intensity in the presence of putrescine (F) subtracted from the intensity in the presence of the same concentration of NaCl as a control (F_0). The wavelength with the maximum change is 340nm. Panel D shows the dependence of $F_0 - F$ at 340nm on the putrescine concentration. The data were fitted to eq 1 to yield a K_d of $150 \pm 20 \mu$ M. Errors are the standard error of the fit. In panel E, the fluorescence F emission change of human AdoMetDC (-) upon addition of 1mM putrescine (---) is shown. In panel F is shown the analysis of putrescine binding to *T. cruzi* AdoMetDC D174V. The fluorescence emission difference ($F_0 - F$) is displayed at 340nm for the titration from 0 to 10mM putrescine.

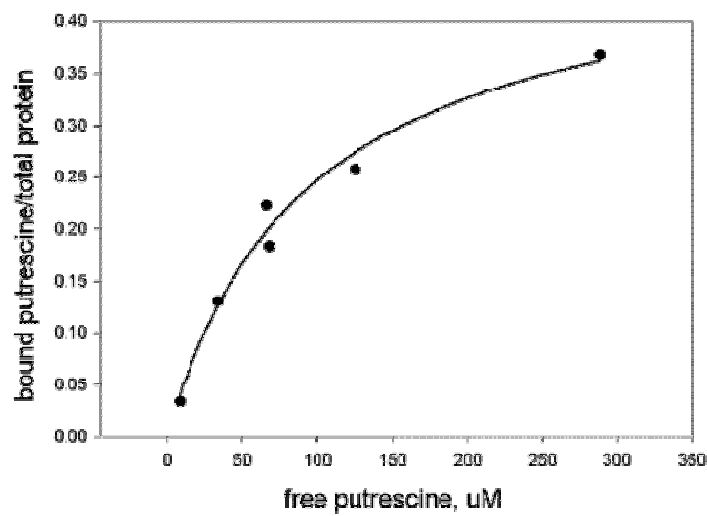


Figure 2.6 Binding analysis of radiolabeled putrescine binding. Equilibrium binding analysis of [^{14}C] putrescine with *T. cruzi* AdoMetDC was performed. The free ligand was separated by ultrafiltration. Data were fitted to eq 2 to determine a K_d of $94 \pm 19 \mu\text{M}$ ($n=0.5$) for this data set, where the errors are the standard error of the fit. The experiment was repeated three independent times, and the average parameters were determined ($K_d = 180 \pm 100 \mu\text{M}$, $n = 1.6 \pm 1.1$), where the error is the standard deviation of the mean.

residue number	human	<i>T. cruzi</i>	plant
13	Leu	Arg	Arg
15	Glu	Glu	Glu
80	Lys	Ile	Lys
111	Phe	Ser	Lys/Arg
113	Ser	Met	Thr
174	Asp	Asp	Met/Val/Ile
176	Thr	Gln	Thr
178	Glu	Ser	Glu
256	Glu	Glu	Glu

Table 2.1 *T. cruzi* and Plant Amino Acid substitutions Identified in the Putrescine Binding Site of Human AdoMetDC. Amino acid residues are numbered on the basis of the human sequence. A multiple-sequence alignment of eukaryotic AdoMetDC enzymes (accession number PF01536) obtained from the PFAM database (Bateman 1999) guided our assignment of structurally equivalent residues for the plant and parasite enzymes. This alignment was compared to the X-ray structure of human AdoMetDC complexed to putrescine to determine the identity of the residues at these positions (Figure 2.1). See Figure 2.1.

putrescine		0 mM		45 mM			
enzyme	$K_d^{\text{Put}}(\text{Fl})$ (μM)	$K_{\text{m,AdoMet}}$ (mM)	k_{cat} (s^{-1})	$K_{\text{m,AdoMet}}^{\text{Put}}$ (mM)	$k_{\text{cat}}^{\text{Put}} (\text{s}^{-1})$	$K_{\text{m,put}}$ (mM)	$k_{\text{cat}}/K_{\text{m}}$ (Put)/ $k_{\text{cat}}/K_{\text{m}}$ (no Put)
wild type	150 ± 10	0.66 ± 0.170	0.018 ± 0.002	0.28 ± 0.06		0.089 ± 0.007	4.7 ± 2.2 11
E15A	8 ± 4	0.96 ± 0.12	0.033 ± 0.002	0.81 ± 0.16		0.047 ± 0.005	7.9 ± 4.5 2
E256A	120 ± 10	2.7 ± 0.9	0.026 ± 0.007	2.0 ± 0.08		0.079 ± 0.002	2.0 ± 0.6 4
I80K/S178E	220 ± 80	4.0 ± 0.5	0.069 ± 0.008	1.0 ± 0.08		0.21 ± 0.009	9.0 ± 2.4 12
D174V	nd	0.73 ± 0.05	0.029 ± 0.001	2.0 ± 0.4		0.064 ± 0.009	nd 0.8

Table 2.2 Summary of Putrescine Binding and Kinetic Analysis of Wild-type and Mutant *T. cruzi* AdoMetDC. $K_d^{\text{Put}}(\text{Fl})$ is the binding constant measured for putrescine by fluorescence as described in the legend of Figure 5. $K_{\text{m,AdoMet}}^{\text{Put}}$ and $k_{\text{cat}}^{\text{Put}}$ are the steady-state parameters for AdoMet in the presence of 45 mM putrescine, and $K_{\text{m,put}}$ is the apparent Michaelis constant for putrescine collected at 0.3 mM AdoMet. nd, not detected. Errors are the standard error of the fit.

Chapter 3

Mechanism of drug selectivity of AdoMetDC using inhibitors CGP 40215 and CGP 48664

A. Introduction

The ability of putrescine to stimulate the activity of the *T. cruzi* and human AdoMetDCs demonstrates these sites are in allosteric communication. To further probe the structural basis for the allosteric communication, we designed 2 classes of mutants of the *T. cruzi* enzyme: those in the putrescine binding site and those in the active site.

Mutations in the putrescine site were designed to make the pocket more like plant AdoMetDC, an enzyme which does not bind putrescine nor utilize it as an activator. These residues include S111R, D174V and F285H and were chosen based on an overlay of the human and potato structures (Figures 1.4, 3.1) as well as sequence alignment (Figure 1.5). *T. cruzi* resembles the human enzyme at these positions, so we mutated these residues to their plant counterparts (S111R, D174V and F285H) in an attempt to make a fully active enzyme in the absence of putrescine.

For active site mutations, sequence alignment (Figure 1.5) and the human AdoMetDC structure complexed with CGP 48664 were used to determine which residues to mutate (Figures 1.5, 3.2). We made mutations of all residues within a 5 Å radius of the inhibitor. This included 7 residues, 5 of which were conserved and mutated to Ala (F7A, V64A, F223A, T245A and E247A); the 2 nonconserved residues were mutated to their human counterparts (A5H and C250F). We also mutated nonconserved residues within 7 Å of the inhibitor (L221T and V52I) to include residues that could possibly contact a larger inhibitor such as CGP 40215. As a final point of interest we sought to determine if the variable residues in the

binding pocket account for the differences in inhibitor potency that are observed for the *T. cruzi* and human enzymes (Table 3.1.)

All mutations were evaluated by comparing effects of putrescine on enzyme activity, but also on the binding of two active site inhibitors, CGP 40215 and CGP 48664. This was done to further explore the mechanism of allostery between the putrescine and active sites. By using two different inhibitors we hope to fully characterize all residues important for drug interactions in the active site. The effects of putrescine on inhibitor binding had not previously been studied for AdoMetDC from any species.

B. Experimental Procedures

1. Materials

S-Adenosyl[carboxyl- ^{14}C]methionine (62mCi/mmol) was purchased from Amersham Pharmacia Biotech (Arlington Heights, IL). Ni^{2+} agarose was purchased from Qiagen Inc. (Chatsworth, CA). QuikChange site-directed mutagenesis kit was purchased from Stratagene (La Jolla, CA). CPG 40215 and CGP 48664 were generous gifts from Novartis. All other reagents were purchased from Sigma.

2. Expression and Purification of AdoMetDC

Both human and *T. cruzi* AdoMetDC were expressed and purified as an N-terminal 6 His-tagged fusion in a T7 bacterial expression construct as previously described (Kinch, Scott et al. 1999). *Escherichia coli* BL21/DE3 cells containing the construct were grown in LB, and the recombinant enzyme was purified using Ni^{2+} agarose column chromatography and anion exchange chromatography. All purification buffers lacked putrescine. The purified protein was quantitated using the extinction coefficient previously determined for the native enzyme (46.5 $\text{mM}^{-1}\text{cm}^{-1}$ for *T. cruzi*, 39.8 $\text{mM}^{-1}\text{cm}^{-1}$ for human).

3. Site-Directed Mutagenesis of *T. cruzi* AdoMetDC

To create mutant AdoMetDC enzymes, PCR-based site-directed mutagenesis using the Stratagene QuikChange kit was performed using the *T. cruzi* AdoMetDC expression plasmid as a template. The constructs were verified by sequencing.

4. Steady-State Kinetic Analysis

Steady-state kinetic analysis of AdoMetDC was performed as previously described (Kinch, Scott et al. 1999). Reactions were carried out in buffer [100mM Hepes, 50mM NaCl, and 5mM DTT] at various AdoMet concentrations. Reaction mixtures were incubated at 37°C for 10, 20 and 40 min at various enzyme concentrations (0.5-8μM for *T. cruzi*, 10nM for human) to ensure a linear rate with time. Data points were typically collected in triplicate. Data were fitted to the Michaelis-Menten equation to determine the rate constants K_m and k_{cat} .

5. Putrescine Activation

Varying amounts of putrescine (0-10mM) were added to enzyme reaction mixtures containing ^{14}C -labeled AdoMet only (34μM) and a set amount of enzyme (varying from 1μM to 8μM depending on the mutant). The data were fitted to the Michaelis-Menten equation to derive a K_d^{app} for putrescine activation.

6. IC₅₀ determination

Varying amounts of CGP 40215 or CGP 48664 (0-10mM) were added to enzyme reaction mixtures containing ^{14}C -labeled AdoMet (various concentrations) only and a set amount of enzyme (varying from 1– 8μM

depending on the mutant). The data were fitted to dose-response curves to determine IC₅₀ values.

C. Results

1. Wild-type *T. cruzi* AdoMetDC kinetics, putrescine stimulation, and inhibition by CGP 40215

Kinetic parameters and putrescine activation have been reported for wild type *T. cruzi* AdoMetDC previously (Table 3.1) (Kinch, Scott et al. 1999). Attempts at reproducing this data worked well for steady state experiments, but titration of putrescine failed to show saturation kinetics, suggesting the K_d was higher than previously observed. To obtain the full range of substrate concentrations needed to accurately determine k_{cat} and K_m, the typical kinetic assay is performed with a mixture of cold and radioactive AdoMet. AdoMet is a highly unstable molecule. It is not sold as a synthetically produced pure compound, but rather is obtained from yeast extract. Thus the purity of this reagent is potentially variable. To determine if impurities in the AdoMet stocks accounted for the lack of reproducibility in the putrescine activation curve, the cold AdoMetDC was left out of the reaction. Under these conditions saturation kinetics with putrescine were observed, giving a K_d of 415μM (Figure 3.3). This is significantly lower than what was previously reported (2.5mM), and the activation at saturating concentration of putrescine is much higher when comparing catalytic efficiencies (27 fold vs. 2.3 fold) (Figures 3.3, 3.4) (Kinch, Scott et al. 1999). We conclude that the cold AdoMet purchased from Sigma is contaminated with a non-UV active small molecule that interferes with putrescine stimulation, and this contamination varies from batch to batch. It is likely to be at least a partial antagonist which can bind the putrescine site since full activation of the enzyme cannot be obtained under conditions that include cold AdoMet. No pure source of cold AdoMet is commercially available and attempts to synthesize

it ourselves have failed. Thus in order to measure the uncompromised effects of putrescine on the system, all further experiments were done with radioactive AdoMet alone (which is synthesized de novo and is thus pure) to avoid this contamination problem.

Using only radioactive AdoMet restricts our experiments to lower substrate concentrations, making determination of the individual parameters k_{cat} and K_m difficult for most mutants. However, the ratio of k_{cat}/K_m can be determined for all cases. For wild type AdoMetDC, k_{cat} and K_m in the absence of cold AdoMet were shown to be 0.0009s⁻¹ and 256μM, respectively (Figure 3.3, Table 3.1). This k_{cat} is roughly 8 fold lower than previously reported, and the K_m is approximately 5 times higher. These differences are most likely attributable to contaminants in the cold AdoMet.

Inhibitor studies using CGP 40215 were undertaken for wild type *T. cruzi* AdoMetDC. Dose response curves done at several substrate concentrations show IC₅₀ values that do not change with increasing substrate concentrations, indicating CGP 40215 is a noncompetitive inhibitor (Figure 4, Table 3.2). For noncompetitive inhibition, K_i equals IC₅₀. The K_i in the absence of putrescine is 32μM; in the presence of 5mM putrescine the K_i decreases to 3μM (figure 2). Thus the effect of putrescine is to enhance the binding of the inhibitor. Because 2μM enzyme was used in the assay, this categorizes CGP 40215 as a tight binding inhibitor under both conditions.

2. Human AdoMetDC kinetics and inhibition by CGP 40215

Using only ¹⁴C labeled AdoMet, human AdoMetDC exhibited a k_{cat} of 1.9s⁻¹ and a K_m of 74μM in the absence of putrescine (Table 3.1). Upon addition of 5mM putrescine, k_{cat} increased to 2.6s⁻¹ and K_m decreased to 59μM (Table 3.1). This translates to a 1.7 fold increase in catalytic efficiency. Previously reported

values for k_{cat} were 0.5s^{-1} and for K_m were $78\mu\text{M}$ in the presence of 0.2mM putrescine (Table 3.1) (Stanley, Shantz et al. 1994). Separately, a 5 fold increase in human AdoMetDC activity was reported upon the addition of 2mM putrescine (Stanley and Pegg 1991). However, this experiment was done with a single concentration of enzyme and a single concentration of substrate so the value may not correspond to maximal activation. Again it is likely that the differences seen between previously reported data and the data presented here are due to contaminants in AdoMet purchased from Sigma.

Titration of CGP 40215 at various AdoMet concentrations are shown in Figure 3.6. CGP 40215 is a tight-binding inhibitor both in the presence ($K_i = 6\text{nM}$) and absence ($K_i = 10\text{nM}$) of 5mM putrescine. It is not surprising that putrescine does not affect the K_i value significantly as it does not affect activity very much either.

When comparing these data for human and *T. cruzi* AdoMetDC, it is easy to see that although these enzymes catalyze the same reaction, the role for putrescine is distinctly different. Upon putrescine addition to the enzyme reaction, the activity of the human enzyme is very modestly increased (~ 2 fold) while *T. cruzi* AdoMetDC sees a 41 fold increase in activity. This distinction was not previously appreciated and could suggest differences in regulation of AdoMetDC activity in a cell. The human enzyme processes slowly, but addition of putrescine increases the processing rate, while the processing rate of *T. cruzi* is unaffected by putrescine (Xiong, Stanley et al. 1997; Clyne, Kinch et al. 2002). Perhaps in human cells control AdoMet decarboxylation by the amount of AdoMetDC that is active (i.e. processed), while trypanosomes control decarboxylation by increasing the activity of the already processed enzyme. It appears both of these cell types have evolved to use putrescine to regulate the activity of AdoMetDC in cells, albeit in different manners.

Another explanation for the lack of putrescine stimulation seen for the human enzyme is that putrescine could be very tightly bound, so adding exogenous putrescine does not help because all the putrescine sites are filled. Putrescine is always bound in crystal structures of human AdoMetDC despite being absent in all purification and crystallization buffers. If this is the case, it would argue that putrescine is capable of regulating the polyamine pathway of *T. cruzi* but not that of the human enzyme.

Although CGP 40215 is a tight binding inhibitor of both *T. cruzi* and human AdoMetDC, they have extremely different affinities for the drug. When comparing the human enzyme to the *T. cruzi* enzyme, the selectivity is 3200 fold in the absence of putrescine and 500 fold when saturating amounts of putrescine are present. This reduction in fold selectivity is entirely due to the reduction in K_i for the *T. cruzi* enzyme under conditions of saturating putrescine.

Additionally, the data suggest this inhibitor is a noncompetitive inhibitor against *T. cruzi* and human AdoMetDC, despite the observation that an analog (CGP 48664) is bound in the active site of the human structure in which putrescine is bound (Tolbert, Ekstrom et al. 2001). However, it is possible to have a noncompetitive inhibitor that binds in or near the active site that occludes substrate binding or prevents product release (Segel 1993). And, CGP 40215 is longer and more flexible when compared to the structure of CGP 48664 (Figure 1.6), so it is possible it only takes up part of the human active site.

3. Analysis of putrescine binding mutants

We made three separate mutations in the predicted putrescine binding site of the *T. cruzi* enzyme to make the enzyme more plant-like (and therefore fully active in the absence of putrescine): S111R, D174V and F285H (Table 3.1). None of those mutations produced a constitutively active enzyme. D174V showed similar catalytic efficiency to wild type. F285H and S111R were 2 fold

and 10 fold less active than wild type in the absence of putrescine, respectively. The fact that S111R is 10 fold less catalytically efficient shows that this position exerts effects on either substrate binding or catalysis from nearly 10 Å away.

K_d s for putrescine were determined for each of the enzymes using a matrix of k_{cat}/K_m data collected at various putrescine concentrations. D174V was not activated at all by putrescine, in keeping with data shown in Chapter 2. The K_d for S111R was 7.9mM, 19 fold higher than wild type. Because this K_d is so high, we determined catalytic efficiency at 30mM putrescine. This showed a slight activation, but this is attributable to activation seen with a comparable ionic strength control, suggesting that S111R is not activated by putrescine (data not shown). Although F285H exhibited a wild type K_d for putrescine, its activity is stimulated to a much greater extent than wild type (353 fold compared to 48 fold, respectively), resulting in an enzyme that is 3 fold more active than the wild type enzyme.

These 3 mutations in the putative putrescine binding pocket shed light on where putrescine could bind in the *T. cruzi* enzyme. The removal of a negative charge at position 174 disrupts putrescine binding, and therefore activation of, *T. cruzi* AdoMetDC. S111R is interesting because instead of being constitutively activated as is observed for plant AdoMetDCs, its activity is 10 fold lower than wild type and it binds putrescine 19 fold more weakly than wild type. According to this data, position 111 is clearly linked to the active site and is likely near the putrescine binding site for *T. cruzi* AdoMetDC because substitution of a positive charge makes putrescine a worse ligand. F285H binds putrescine similarly to wild type but exhibits much stronger activation of decarboxylation. Although this suggests that putrescine does not bind near position 285, it does show that position 285 communicates with the active site and could be important for putrescine stimulation of activity. Additionally, the facts that plant AdoMetDCs

have H285 and are fully active in the absence of putrescine are consistent with this.

To probe the interaction between putrescine activation and inhibition by CGP 40215, the three putrescine mutants were assayed to determine K_i . In the absence of putrescine, K_i values for D174V and F285H were the same as wild type while S111R showed a 3 fold higher K_i . However, in the presence of 5mM putrescine, K_i values for D174V and S111R did not change, unlike wild type which decreased 10 fold. The K_i for F285H was decreased 25 fold in the presence of putrescine, similar to the activation of binding seen for wild type. These data show that mutations that disrupt the putrescine site (S111R and D174V) also prevent the ability of putrescine to decrease K_i . Thus mutations that disrupt the ability for the enzyme to bind putrescine result in an enzyme that cannot be fully activated for substrate catalysis or potent inhibitor binding.

4. Analysis of active site mutations

Catalytic efficiencies of all the active site mutants were determined and are summarized in Table 3.4. In the absence of putrescine, F7A, V64A, T245A, E247A and C250F are at least 5 fold less catalytically efficient than wild type *T. cruzi* AdoMetDC, indicating these residues may have a modest role in substrate binding or catalysis. F7A is virtually dead, which is not unexpected. According to its position in the human structure, F7A, along with F223 (a residue that, when mutated, did not express), are involved in ring stacking interactions with the adenosyl moiety of the substrate (Tolbert, Ekstrom et al. 2001).

K_{ds} for putrescine were determined for each of the enzymes using a matrix of k_{cat}/K_m data collected at various putrescine concentrations. All active site mutants showed K_{ds} similar to wild type, suggesting that mutations at these positions do not affect putrescine binding to *T. cruzi* AdoMetDC. However, most active site mutants did not achieve wild type levels of putrescine activation of the

catalytic efficiency. Mutants that exhibit at least 5 fold less activation include A5H, F7A, V64A, and T245A. F7A, V64A and T245A were less active than wild type with or without putrescine. However, A5H was relatively normal in the absence of putrescine, but upon addition of putrescine shows only 7 fold activation. This indicates position 5 could be important for relaying information from the putrescine site to the active site.

CGP 40215 inhibition of the active site mutants is described in Table 3.2. Enzymes with higher K_i values are V64A, T245A and E247A. All three of these were also low in activity. Addition of putrescine was able to decrease the K_i values for these mutants, although it was incapable of completely reducing them to wild type levels. Interestingly, L221T had a 32 fold lower K_i than wild type in the absence of putrescine. This *T. cruzi* to human change could partially explain why the human enzyme shows stronger inhibition with CGP 40215 than wild type *T. cruzi* AdoMetDC. Also, the addition of putrescine to L221T did not affect K_i , whereas the wild type *T. cruzi* enzyme shows a 10 fold decrease in K_i upon the addition of putrescine. This is another point where the L221T mutant exhibits more human-like characteristics, as the CGP 40215 K_i for the human enzyme is relatively unaffected by addition of putrescine as well.

5. CGP 48664 inhibition of various AdoMetDCs

As mentioned above, we tested two related inhibitors against human and *T. cruzi* AdoMetDC in hopes of fully characterizing which active site residues are important for drug binding and potency. The second of these tested, CGP 48664, displayed different inhibitory patterns than CGP 40215. The human enzyme is noncompetitively inhibited by CGP 48664 with K_i values of 5.4nM and 3.3nM in the absence and presence of 5mM putrescine, respectively (data not shown). This lack of putrescine strengthening of inhibition is similar to the human enzyme's response to CGP 40215.

T. cruzi AdoMetDC, however, showed a distinct response to CGP 48664 inhibition. At lower drug concentrations, activity was actually increased. As more inhibitor was titrated in, inhibition was finally seen with an estimated IC_{50} of 100 μ M (figure 3.7A). This effect is greater for E247A and is completely abolished in D174V (Figure 3.7B). The addition of putrescine to both wild type and E247A abrogated the activation effect and allowed determination of IC_{50} values (4.4-6.9 μ M and 140 μ M, respectively). CGP 48664 exhibited noncompetitive inhibition for all *T. cruzi* AdoMetDC enzymes tested.

The unusual inhibition pattern of CGP 48664 was unexpected. This inhibitor was complexed with human AdoMetDC for crystallographic studies and was bound in the active site (Tolbert, Ekstrom et al. 2001). Therefore we assumed CGP 48664 would demonstrate straightforward competitive inhibition. It is possible, as with the CGP 40215 inhibitor, that although CGP 48664 is bound in the active site, substrate can somehow share the space. In this case CGP 48664 would exhibit noncompetitive inhibition by preventing substrate binding and/or product release (Segel 1993).

A possible explanation for CGP 48664 activation kinetics is allostery between active sites of dimers in which an equilibrium exists between active and inactive conformations of the enzyme, per the Monod, Wyman and Changeux model ((Voet 1995). A classic example of this type of allostery is observed for the binding of PALA to ATCase (Voet 1995). Another explanation is that CGP 48664 is capable of binding both the putrescine binding site and the active site, and that it functions as an activator when bound in the putrescine site.

Future experiments to address these hypotheses include crystallizing *T. cruzi* AdoMetDC with CGP 48664 bound. This would clear up not only where CGP 48664 binds but also how many molecules bind per monomer of enzyme. It would also show the oligomerization state of the molecule. However, several labs have been working on crystallizing the trypanosomal form of the enzyme without

any success as of yet. Another experiment to determine how many molecules of CGP 48664 bind per monomer of AdoMetDC would be isothermal calorimetry. This could be combined with mutation studies to determine exactly where the inhibitor binds.

D. Discussion

Using radioactive AdoMet alone to avoid contamination in activity assays allowed us to see the full activation of both human and *T. cruzi* AdoMetDC. Previously, it was thought that the *T. cruzi* enzyme showed only a 9 fold activation upon putrescine addition; now, activation is approximately 40 fold. In comparison to this data, the activation of the human enzyme is very modest, at best ranging from 2-5 fold (Stanley and Pegg 1991). This disparity in activation is also carried over into the inhibitor studies. The ability of both CGP 40215 and CGP 48664 to inhibit *T. cruzi* AdoMetDC was enhanced by the addition of putrescine, while addition of putrescine to the human enzyme showed negligible effects on K_i . This difference in putrescine's ability to enhance decarboxylation and inhibition suggests that the method by which putrescine communicates to the active site is vastly different for both enzymes. This is also seen in the processing reaction, which is stimulated by putrescine for human AdoMetDC but not for the *T. cruzi* enzyme. It appears that although both enzymes have evolved to bind putrescine, each has tailored putrescine stimulation to control a different checkpoint in the polyamine pathway. For human AdoMetDC, the point of putrescine control is at the step of making mature enzyme. Trypanosomes use putrescine to control the pathway by stimulating decarboxylase activity. The difference in putrescine stimulation coupled with the difference in affinity for CGP 40215 and CGP 48664 (approximately 1000 fold lower K_i for the human enzyme) highlights the fact that these enzymes function differently enough to develop species specific inhibitors.

In order to probe the putative putrescine binding site and its communication with the active site, we made mutations to make the *T. cruzi* enzyme more like the plant enzyme. We did not succeed in creating a fully activated enzyme. However, introduction of a positive charge at position 111 lessened decarboxylase activity and severely weakened the ability of putrescine to bind, and mutation of 285 to a positively charged residue produced an enzyme capable of being more activated upon addition of putrescine. The effects seen upon putrescine stimulation for S111R, D174V and F285H argue that these residues are close to the putrescine binding site for *T. cruzi* AdoMetDC. Additionally, these mutants show positions 111 and 285 are important for communicating to the active site even though they are approximately 10Å away.

The above data, combined with the R13L mutation and data collected for mutants known to disrupt putrescine stimulation of activity for the human enzyme provide insight to the location of the putrescine binding site in *T. cruzi* AdoMetDC. *T. cruzi* and plant both share Arg at position 13, and in the plant AdoMetDC structure, the sidechain of R13 would sterically and electrostatically interfere with the position of the putrescine in the human enzyme (Figure 3.1). This argues that putrescine does not bind in this area in the *T. cruzi* enzyme. D174, however, is a residue that both *T. cruzi* and human AdoMetDC have in common, and both enzymes fail to respond to putrescine when this Asp is mutated (Stanley and Pegg 1991)(Chapter 2). This residue is on the outer surface of the protein, and its negatively charged sidechain is capable of interacting with the positively charged amino group on the end of putrescine. Additionally, mutations F285H and S111R are very close to position 174, and those mutants showed effect on putrescine binding or stimulation of activity. Taken together, these data argue for a putrescine binding site in *T. cruzi* that is more on the outer surface of the protein when compared to the human putrescine site.

The active site mutations in *T. cruzi* AdoMetDC were created to see which residues were important for inhibitor binding and to determine which residues that differed between human and *T. cruzi* enzymes were responsible for potency. Residues V64, T245 and E247 all had increased K_i values; thus, they are important for inhibitor binding. Also, these residues are all on the same side of the active site pocket, indicating that the inhibitor might bind near that surface, leaving room for substrate to bind on the opposite face of the active site.

L221T, a humanizing mutation, showed increased affinity for CGP 40215 (40 fold in the absence of putrescine), and the inhibition was not strengthened when putrescine was added. This residue is deep in the active site pocket and could potentially make contact with a large inhibitor such as CGP 40215. In the absence of putrescine, the K_i values for L221T and human AdoMetDC are 800nM and 51nM, respectively. This mutation might reduce a steric clash that partially accounts for why the *T. cruzi* enzyme binds the inhibitor with lower affinity than the human enzyme. Additionally, since CGP 40215 inhibition of L221T is not strengthened by the addition of putrescine, position 221 must be important for allostery between the putrescine site and the inhibitor binding site. Additionally, humanizing mutation A5H significantly lessened putrescine's ability to enhance decarboxylation and inhibition by CGP 40215. This residue could be important for the difference seen in putrescine stimulation between the two enzymes.

Another interesting aspect of putrescine's effects on *T. cruzi* AdoMetDC is the difference in stimulation of catalysis and inhibition. When 5mM putrescine is added, catalysis is stimulated 27 fold whereas inhibition by CGP 40215 is enhanced only 10 fold. This supports the idea that the inhibitor is binding in a separate space in the active site than the substrate. Most mutants followed this same trend of putrescine affecting catalysis more than inhibition. Exceptions to this include mutants F7A, V64A, T245A and E247A, all of which have inhibition strengthen more than activity upon the addition of putrescine. These enzymes are

much less active than wild type in the absence of putrescine, and putrescine is incapable of rescuing this inactivity. Of these, F7A is the only one that exhibits inhibition similar to wild type. V64A, T245A and E247A have much higher K_i s than wild type in the absence of putrescine, but when putrescine is added these mutants see a significant decrease in K_i . This argues that V64, T245 and E247 are not only important for substrate binding but also for communication between the putrescine site and the part of the active site where CGP 40215 binds. The fact that different mutants disrupt the allostery of activation and inhibition differently support the theory that CGP 40215 is binding in a different area of the active site than the substrate.

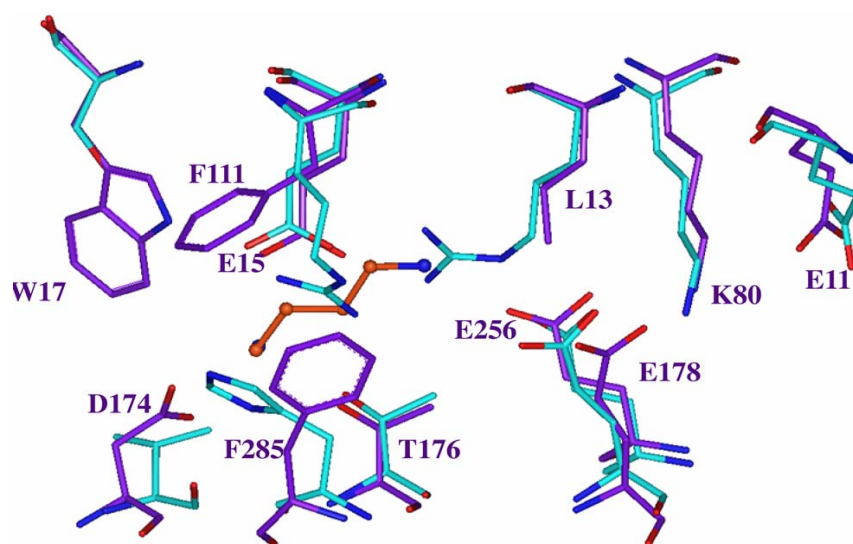


Figure 3.1 Overlay of putrescine binding site of human and potato AdoMetDC structures. Putrescine is in red, the human enzyme is in purple and the potato enzyme is in cyan. The figure was created in InsightII from pdb files 1I7M and 1MHM (Tolbert, Ekstrom et al. 2001; Bennett, Ekstrom et al. 2002).

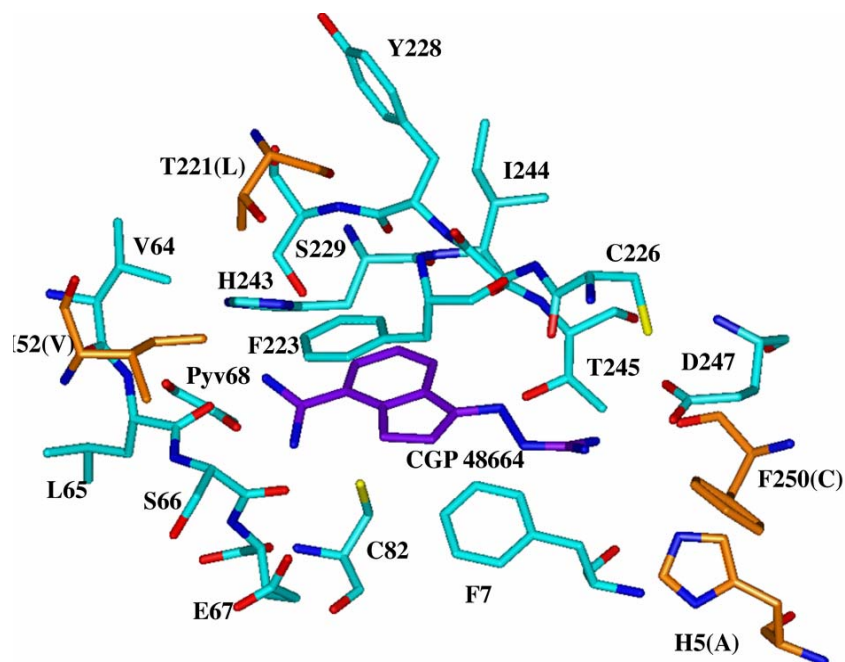


Figure 3.2 Active site of human AdoMetDC (cyan) with the inhibitor CGP 48664 (purple) complexed. Residues in orange are in the 7Å shell, and letters in parenthesis represent the analogous residue in *T. cruzi* AdoMetDC. Figure was made in InsightII using the PDB file 1I7M (Tolbert, Ekstrom et al. 2001).

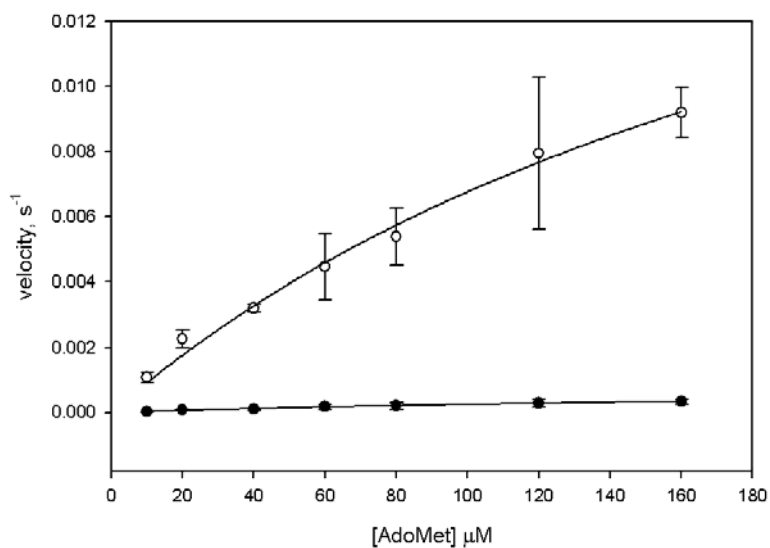


Figure 3.3. Substrate titration of 1 μM wild type *T. cruzi* AdoMetDC, in the presence (open circles) or absence (closed circles) of 5mM putrescine. Error bars are standard error of the mean. No putrescine $K_m = 256 \pm 76 \mu\text{M}$, $k_{cat} = 0.0009 \pm 0.0002 \text{ s}^{-1}$. 5mM putrescine $K_m = 245 \pm 61 \mu\text{M}$, $k_{cat} = 0.0234 \pm 0.004 \text{ s}^{-1}$. Errors for kinetic parameters are standard error of the fit.

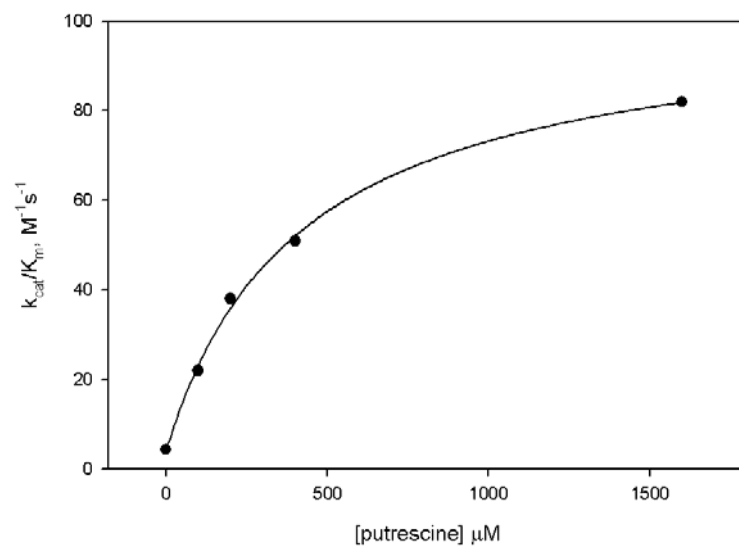


Figure 3.4. Putrescine titration of 1 μM *T. cruzi* AdoMetDC with 32 μM radioactive AdoMet.

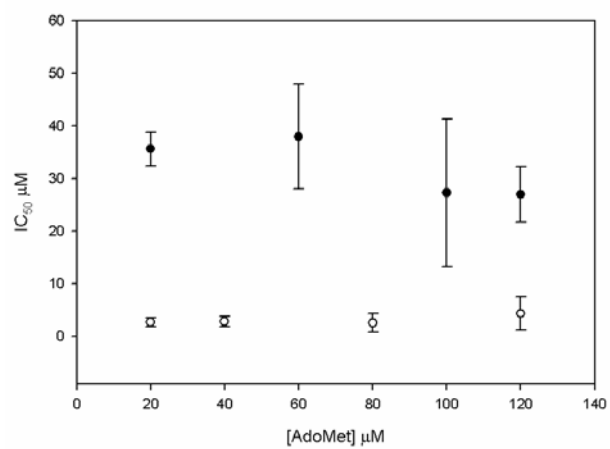


Figure 3.5 IC₅₀ data for wild type *T. cruzi* AdoMetDC indicate that CGP 40215 is a noncompetitive inhibitor. No putrescine $K_i = 32\mu\text{M}$ (closed circles). 5mM putrescine, $K_i = 3\mu\text{M}$ (open circles). Errors are standard deviations for 3 separate experiments.

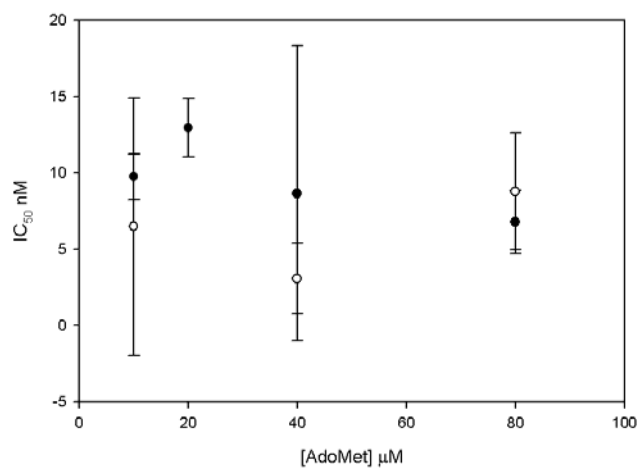
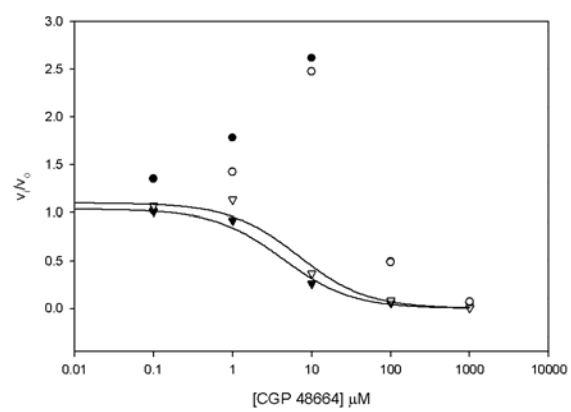
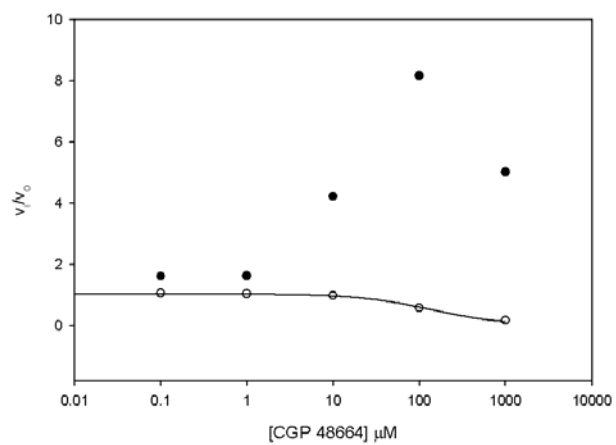


Figure 3.6 IC_{50} data for human AdoMetDC indicate that CGP 40215 is a noncompetitive inhibitor. No putrescine $K_i = 10$ nM (closed circles). 5mM putrescine, $K_i = 6$ nM (open circles). Errors are standard deviations for 3 separate experiments.

A)



B)



C)

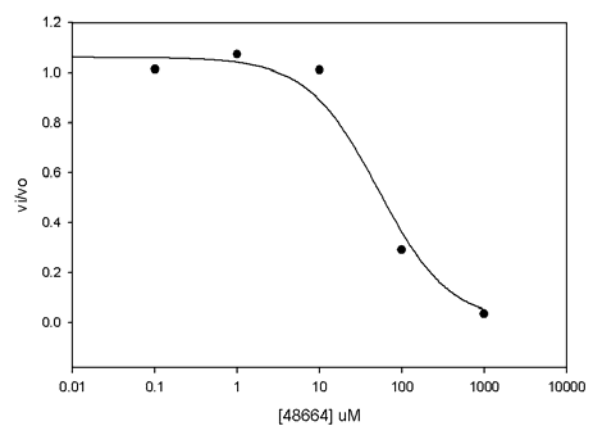


Figure 3.7 CGP 48664 dose response curve for A) wild type B)E247A and C) D174V *T. cruzi* AdoMetDC in the presence and absence of 5mM putrescine. For A), circles = no putrescine, triangles = 5mM putrescine. Open symbols were collected at 10 μ M AdoMet and closed symbols are data collected at 80 μ M AdoMet. IC₅₀ values for wild type in the presence of putrescine are 4.4 μ M and 6.9 μ M for 10 μ M and 80 μ M AdoMet, respectively. IC₅₀ values for wild type in the absence of putrescine are estimated to be 100 μ M in the absence of putrescine. For B) and C) closed circles = no putrescine, open = 5mM putrescine. IC₅₀ values are 140 μ M for E247A in the presence of 5mM putrescine and 42 μ M for D174V in the absence of putrescine.

	Previous data					New data				
	0mM putrescine		5mM putrescine		fold activation	0mM putrescine		5mM putrescine		fold activation
	k_{cat} , s^{-1}	K_m , μM	k_{cat} , s^{-1}	K_m , μM	k_{cat}/K_m $M^{-1}s^{-1}$	k_{cat} , s^{-1}	K_m , μM	k_{cat} , s^{-1}	K_m , μM	k_{cat}/K_m , $M^{-1}s^{-1}$
<i>T. cruzi</i>	0.007	50	0.06	100	4.3	0.0009	256	0.0234	245	27
Human	N.D.	312	0.481	78	N.D.	1.9	74	2.6	59	1.7

Table 3.1 Summary of previously determined and new data on activity of human and *T. cruzi* AdoMetDCs in the presence and absence of putrescine. Previous data were collected using cold and radioactive AdoMet (Stanley, Shantz et al. 1994; Kinch, Scott et al. 1999). New data were collected using radioactive AdoMet alone. N.D. (not determined) – k_{cat} in the absence of putrescine was not determined in (Stanley, Shantz et al. 1994).

	CGP 40215 K_i		
	0mM putrescine	5mM putrescine	fold stimulation
<i>T. cruzi</i>	32 +/- 6 μ M	3.2 +/- 0.8 μ M	10
Human	10 +/- 3 nM	6.1 +/- 2.9 nM	1.7

Table 3.2 K_i values for CGP 40215 against human and *T. cruzi* AdoMetDCs in the presence (5mM) or absence of putrescine. Values were obtained by collecting IC_{50} s at 10, 20, 40 and 80 μ M AdoMet and averaging the 4 different IC_{50} s. Error is the standard deviation of these averages.

enzyme	k_{cat}/K_m , no putrescine ($M^{-1}s^{-1}$)	k_{cat}/K_m , 5mM putrescine ($M^{-1}s^{-1}$)	fold activation	K_d putrescine (μM)	K_i , no putrescine (μM)	K_i , 5mM putrescine (μM)
wt	5	203	41	417+/-51	32+/-6	3.2+/-0.8
S111R	0.4	N.D.	N.D.	7900+/- 2600	96+/-24	104+/-48
D174V	6.6	5	1	none	13+/-4	14+/-5
F285H	1.8	635	353	316+/-59	26+/-11	1.2+/-1.2

Table 3.3 Kinetic parameters for wild type and putrescine binding mutants of *T. cruzi* AdoMetDC. N.D. = not determined. K_d errors are standard errors of the fit. K_i values are the average of IC_{50} s (CGP 40215) determined at 3 different substrate concentrations (10, 32 and 80 μM). K_i errors are standard deviations of the mean.

enzyme	k_{cat}/K_m , no putrescine ($M^{-1}s^{-1}$)	k_{cat}/K_m , 5mM putrescine ($M^{-1}s^{-1}$)	fold activation	K_d putrescine (μM)	CGP 40215 K_i , no putrescine (μM)	CGP 40215 K_i , 5mM putrescine (μM)	fold stimulation of binding
wt	5	203	41	420+/-50	36+/-6	3.2+/-0.8	11
A5H	2	14	7	210+/-120	13+/-3	5+/-5	3
F7A	0.1	0.6	6	320+/-60	26+/-6	7+/-0	4
V52I	4	94	24	340+/-270	18+/-6	4+/-4	5
V64A	0.5	4	8	790+/-400	150+/-40	13+/-10	12
L221T	2	31	16	440+/-40	0.8+/-0.9	0.8+/-0.5	1
T245A	0.9	3	3	530+/-50	440+/-100	34+/-13	13
E247A	0.2	4	20	330+/-150	4100+/-680	88+/-78	46
C250F	1	14	14	470+/-100	28+/-8	4+/-2	7

Table 3.4. Kinetic data for wild type and active site mutations of *T. cruzi* AdoMetDC. Errors on K_d are standard errors of the fit.

Chapter 4

Yeast complementation/selection with inhibitors using mutated *T. cruzi* AdoMetDC

A. Introduction

For drug discovery purposes, it is useful to find differences between human and *T. cruzi* AdoMetDC. The previous chapters have shown that human and trypanosomal AdoMetDC respond differently to various inhibitors. In order to determine the structural basis for species specific selectivity of inhibitors, we implemented a random mutagenesis approach. We hoped this would allow us to find mutations that affect inhibition that might not be inherently obvious by using structure and sequence alignments, including amino acid positions that are far removed from the inhibitor binding site. Evidence for a distant site that affects activity already exists for human AdoMetDC. Mutation of Y112, R114, H127 and E133 yields enzymes that are much less active than wild type (Ekstrom, Mathews et al. 1999). This cluster of residues is not near the putrescine binding site, the dimer interface or the active site and yet it still somehow affects activity.

To achieve random mutagenesis of the *T. cruzi* AdoMetDC gene, we planned on using PCR based random mutagenesis (such as GeneMorphII by Stratagene) or DNA shuffling (Stemmer 1994). Some examples of protein evolution by PCR random mutagenesis include increasing the protein stability of congerin II (Shionyu-Mitsuyama, Ito et al. 2005) and increasing the catalytic efficiency of *T. brucei* triosephosphate isomerase (Saab-Rincon, Juarez et al. 2001).

DNA shuffling begins with enzymatic digestion of homologous genes, producing small fragments of DNA. These small fragments then are allowed to reassemble at random in a primerless PCR reaction and then the full-length sequences are amplified. For our experiments, the human and *T. cruzi*

AdoMetDC genes would be used. Conversion of the enzyme β -galactosidase to β -fucosidase (Zhang, Dawes et al. 1997) and thermostabilization of fructose bisphosphate aldolase (Hao and Berry 2004) are examples of protein engineering accomplished by DNA shuffling.

We developed yeast complementation/selection in which randomly mutagenized *T. cruzi* AdoMetDC is transformed into $\Delta spe2$, a yeast strain that is auxotrophic for AdoMetDC activity when grown on media not containing polyamines or pantothenic acid (White, Gunyuzlu et al. 2001) (Figure 5.1). The transformed yeast would then be exposed to CGP 40215, a known AdoMetDC inhibitor. In this selection, the yeast that live in the presence of drug should have a *T. cruzi* AdoMetDC that is still functional but now drug resistant. Similar, successful studies have been done with human β -secretase, *Toxoplasma gondii* dihydrofolate reductase, and malarial mefloquine resistance genes (Reynolds, Oh et al. 2001; Middendorp, Ortler et al. 2004; Jeffress and Fields 2005).

B. Experimental Procedures

1. Yeast strains

$\Delta spe2$ (MAT α his3 Δ 1 leu2 Δ 0 lys2 Δ 0 ura3 Δ 0 spe2 Δ) and $\Delta erg6$ (MAT α Δ his3 Δ 1 leu2 Δ 0 met15 Δ 0 ura3 Δ 0 erg6 Δ) strains were purchased from ATCC.

2. Cloning of *T. cruzi* and human AdoMetDC genes into yeast expression vector

The full length *T. cruzi* AdoMetDC gene was attained by PCR using the previously described construct (Kinch, Scott et al. 1999) as a template with primers TcSamHindf (5'-CCCAAGCTTATGTTAAGCAATAAGGACCC-3') and TcSamNotstop (5'-

ATAAGAATGCGGCGGCCTACTCTTCCACAGAATCTG-3'). The PCR product and the yeast expression vectors from the YES series by Invitrogen (pYES2/CT and pYC2/CT) were digested with HindIII and NotI. The two fragments were isolated and then ligated to form the yeast expression vectors Tsam.YES and Tsam.YC. The constructs were verified by sequencing. The YES series of vectors have URA3 selectable marker, GAL1 promoter and CYC1 terminator and are ampicillin resistant. pYES2/CT is a 2um plasmid and pYC2/CT is a CEN plasmid.

The human AdoMetDC gene was attained by PCR using pSam13 as a template and the primers HSamHindf (5'-CCCAAGCTTATGGAAGCTGCACATTTTTC-3') and HSamNotstop (5'-ATAAGAATGCGGCCGCTCAACTCTGCTGTTGTTGC-3'). Cloning of this gene into the yeast expression vectors was the same as above.

3. Determination of IC₅₀ value for CGP 40215

T. cruzi AdoMetDC was expressed and purified as described previously (Kinch, Scott et al. 1999). The purified enzyme was assayed as described previously (Kinch, Scott et al. 1999). Briefly, enzyme was added to a mixture of buffer (100mM Hepes pH 8.0, 50mM NaCl and 5mM DTT), 0.3mM AdoMet, 10mM putrescine and varying concentrations of CGP 40215 (0.002 – 19mM). The assay was conducted at 37° C for 10 min, at which time the reaction was stopped by adding 0.2ml 6M HCl. Reaction velocities were calculated and the data were fitted using Sigma Plot.

4. Transformation of the *T. cruzi* AdoMetDC yeast vector into Δ spe2 cells

The Δ spe2 strain was grown in 25ml of YPD in a 30° C shaker overnight. In the morning the culture was checked for contamination and an OD

was taken. 8.3 OD of the culture was pelleted at 3000xg for 5min. The pellet was resuspended in 50ml YPD and incubated in a 30° C shaker for 4 hours. The culture was pelleted at 3000xg for 5min. The pellet was resuspended in sterile water and centrifuged again. The pellet was resuspended in 700ul 100mM LiAc. The cells were pelleted at top speed for 15 seconds and the LiAc was removed with a pipette. The cells were resuspended in 370µl of 100mM LiAc. The suspension was vortexed and aliquoted into 50µl samples. Each aliquot was pelleted at top speed for 15 seconds and the LiAc removed with a pipet. 240µl PEG 3350 (50% w/v), 36ul 1M LiAc, 25µl single stranded DNA (HSD 2mg/ml, previously boiled for 5 min) and 50µl water with 5µg of either Tsam.YES or Tsam.YC were carefully added in that order. Each transformation tube was vortexed vigorously until the pellet was completely resuspended. The tubes were then incubated at 30° C for 30 min and then 42° C for 30 min, all the while gently shaking. The samples were then microfuged at 7000rpm for 15 seconds and the transformation mix was removed gently with a pipette. 587µl of sterile water was pipetted into each tube and the pellet resuspended by pipetting up and down gently. 30µl was transferred into 70µl sterile water and plated on SCGal-ura plates (made with galactose as a carbon source instead of glucose because expression of *T. cruzi* AdoMetDC is driven by the GAL1 promoter).

5. Growth of transformants on minimal media

Δspe2 transformed with either Tsam.YES or Tsam.YC grown on SCGal-ura plates was restreaked onto YNBGal-P-ura plates (YNB media with galactose instead of glucose, without pantothenic acid or uracil) and incubated for 3-4 days at 30° C.

C. Results and discussion

1. Cloning of *T. cruzi* AdoMetDC gene into yeast expression vectors

The overall goal of this experiment is to determine if mutations at distant sites will affect the ability of CGP 40215 to inhibit *T. cruzi* AdoMetDC. The assay to determine if inhibition occurs or has been overcome by mutation is to transform mutated *T. cruzi* AdoMetDC into a yeast strain lacking its own AdoMetDC (yeast strain $\Delta spe2$). When this strain is grown on a special minimal media (YNBGal-P-ura), it is auxotrophic for AdoMetDC activity. So, the first step in this experiment is to determine if *T. cruzi* AdoMetDC is capable of rescuing the phenotype of $\Delta spe2$ cells when grown on YNBGal-P-ura. In order to do that, the *T. cruzi* gene was cloned into two different expression vectors that carry a GAL promoter region. Two vectors were chosen, pYES/CT (2 μ m) and pYC/CT (CEN). 2 μ m plasmids have approximately 20 copies of the plasmid per cell, while CEN plasmids have only one copy per cell. Because we did not know how much *T. cruzi* AdoMetDC would be required to overcome the auxotrophy of the $\Delta spe2$ strain, both vectors were used as a way to control how much *T. cruzi* AdoMetDC is expressed in the cell.

2. Determination of IC₅₀ value of CGP 40215 for *T. cruzi* AdoMetDC

MGBG is a potent inhibitor of human AdoMetDC, although it is nonspecific in that it inhibits other cellular targets as well. In hopes of creating specificity, several MGBG analogs were created; CGP 40215 is one of these. IC₅₀ values of 5nM have been reported for both *O. volvulus* and human AdoMetDC. Determination of *T. cruzi* AdoMetDC IC₅₀ for CGP 40215 was undertaken in order to have an idea of the drug concentration required to use in our plates for our selection experiment. *T. cruzi* AdoMetDC has a much higher IC₅₀ for MGBG than the human enzyme, so the IC₅₀ of CGP 40215 was expected to be higher as well. Indeed, the IC₅₀ for *T. cruzi* AdoMetDC was 5 μ M. This is 1000 fold higher than the human AdoMetDC IC₅₀.

3. Growth of transformants on YNBGal-P-ura plates

Transformation of Tsam.YES and Tsam.YC into $\Delta spe2$ cells was confirmed by plating on SCGal-ura plates. Colonies from these plates were then transferred to YNBGal-P-ura to determine whether Tsam.YES or Tsam.YC could compensate for the lacking yeast AdoMetDC gene in $\Delta spe2$ cells. After 6 day incubation at 30° C, growth was seen for both Tsam.YES and Tsam.YC transformants but not for vector only controls, confirming that the *T. cruzi* AdoMetDC gene is capable of producing enough dcAdoMet to rescue the phenotype. To ensure that the selection was due to inhibition of AdoMetDC, we added 250 μ M spermine to the YNBGal-P-ura plates to see if it could rescue the phenotype of $\Delta spe2$ cells transformed with vector alone. Indeed, the vector-only controls grew, suggesting we were working with the correct strain. Upon addition of 10 μ M CGP 40215 to the minimal media, the Tsam.YES and Tsam.YC transformants still grew. All transformants grew under conditions of added drug and spermine.

Because Tsam.YES and Tsam.YC transformants were capable of growth on minimal media plates with 10 μ M drug, the concentration of drug on the plates was increased to see if we could find a dose that would kill the transformants. Concentrations as high as 320 μ M were incapable of killing the yeast. There are several possible reasons for this: 1) the drug has a short half life and is now inactive, 2) the drug was degraded when added to hot agar, 3) we are still not at high enough concentrations of drug to inhibit the *T. cruzi* AdoMetDC gene and 4) the drug does not enter the yeast cell.

To test the first hypothesis, CGP 40215 was tested again against purified *T. cruzi* AdoMetDC in an enzyme assay, and the same IC₅₀ was determined. To ensure the drug was not degraded by addition to hot agar, we let the agar cool to

50° C before adding the drug. Transformants still grew. For the third hypothesis, we cloned human AdoMetDC into the YES and YC vectors and transformed each vector into *Δspe2* cells. Because the human enzyme has a much lower IC₅₀ it should be easier to inhibit this enzyme with less drug on the plate. However, CGP 40215 concentrations up to 100μM failed to prevent *Δspe2* transformed with human AdoMetDC from growing.

This leads us to our last hypothesis, that CGP 40215 is incapable of entering the yeast cell. For compounds to enter a yeast cell, they must be able to pass through its cell wall and membrane. The cell wall is relatively permeable to small molecules; its primary objective is to keep things with large molecular weight (i.e. proteins) out of the cell. However, just in case CGP 40215 was unable to get through the cell wall, we tried spheroblasting *Δspe2* transformants. Unfortunately, spheroblasting produced no viable transformants.

To address the issue of the yeast cell membrane permeability to CGP 40215, we ordered a *Δerg6* strain. This strain is missing a gene in the ergosterol pathway. Ergosterol is an important steroid in the yeast cell membrane, and lack of ergosterol has been shown to increase cell membrane permeability to certain drugs (Jensen-Pergakes, Kennedy et al. 1998). *Δerg6* was capable of growth on YPD in the presence and absence of 100μM drug, as it should have been. When 100μM CGP 40215 was added to minimal media plates (that would require a functional, uninhibited AdoMetDC for growth), the *erg6* knockout was incapable of growth. However, this was not rescued by addition of spermine, suggesting some reason other than an inactive AdoMetDC was the cause for lack of growth. *Δerg6* has been shown to grow better on media supplemented with more amino acids, so casamino acids were added to the media and still the *Δerg6* was incapable of growth.

If the $\Delta erg6$ strain had shown increased permeability to CGP 40215, we would have made a $\Delta spe2, \Delta erg6$ strain. Unfortunately, given the difficulty in growing the $\Delta erg6$ strain, we decided to stop experiments there.

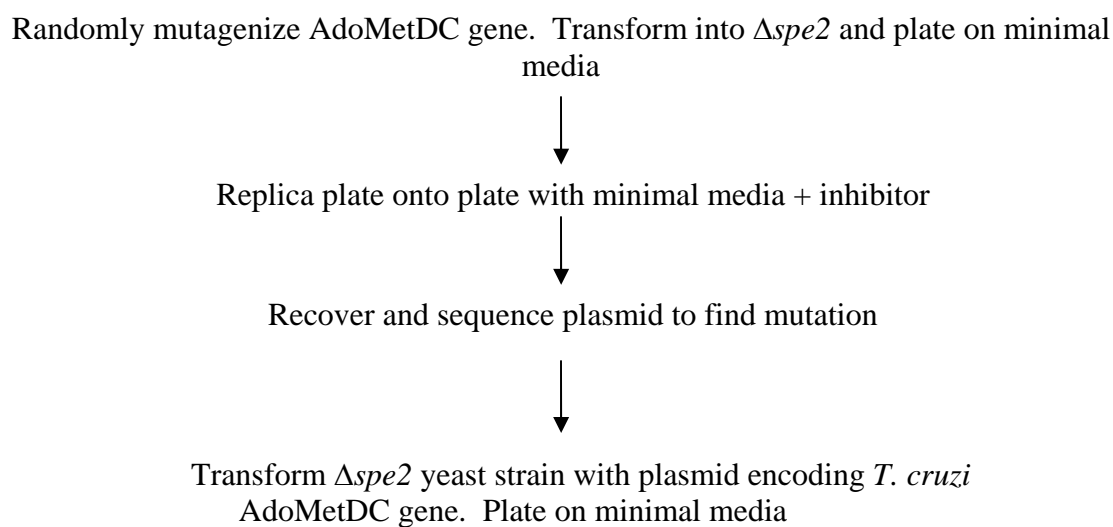


Figure 4.1 Schematic of the proposed *T. cruzi* AdoMetDC yeast complementation/selection using inhibitor CGP 40215 and a $\Delta spe2$ yeast strain.

REFERENCES

- Bacchi, C. J., R. Brun, et al. (1996). "In vivo trypanocidal activities of new S-adenosylmethionine decarboxylase inhibitors." Antimicrob Agents Chemother **40**(6): 1448-53.
- Bacher, J. M., B. D. Reiss, et al. (2002). "Anticipatory evolution and DNA shuffling." Genome Biol **3**(8): REVIEWS1021.
- Barry, J. D. and R. McCulloch (2001). "Antigenic variation in trypanosomes: enhanced phenotypic variation in a eukaryotic parasite." Adv Parasitol **49**: 1-70.
- Bateman, A., Birney, E., Durbin, R., Eddy, S.R., Finn, R.D., and Sonnhammer, E.L. (1999). "Pfam 3.1: 1313 multiple alignments and profile HMMs match the majority of proteins." Nucleic Acids Research **27**: 260-262.
- Bennett, E. M., J. L. Ekstrom, et al. (2002). "Monomeric S-adenosylmethionine decarboxylase from plants provides an alternative to putrescine stimulation." Biochemistry **41**(49): 14509-17.
- Borch, R. F., Bernstein, M.D., and Durst, H.D. (1971). "The cyanobohydridoborate anion as a selective reducing agent." Journal of the American Chemical Society **93**: 2896-2904.
- Brun, R., Y. Buhler, et al. (1996). "In vitro trypanocidal activities of new S-adenosylmethionine decarboxylase inhibitors." Antimicrob Agents Chemother **40**(6): 1442-7.
- Brun, R., C. Burri, et al. (2001). "The story of CGP 40 215: studies on its efficacy and pharmacokinetics in African green monkey infected with *Trypanosoma brucei rhodesiense*." Trop Med Int Health **6**(5): 362-8.
- Choi, Y. S. and Y. D. Cho (1994). "A new S-adenosylmethionine decarboxylase from soybean axes." Biochim Biophys Acta **1201**(3): 466-72.
- Clyne, T., L. N. Kinch, et al. (2002). "Putrescine activation of *Trypanosoma cruzi* S-adenosylmethionine decarboxylase." Biochemistry **41**(44): 13207-16.

Da'dara, A. A., H. Mett, et al. (1998). "MGBG analogues as potent inhibitors of S-adenosylmethionine decarboxylase of *Onchocerca volvulus*." Mol Biochem Parasitol **97**(1-2): 13-9.

Dorhout, B., M. F. Odink, et al. (1997). "4-Amidinoindan-1-one 2'-amidinohydrazone (CGP 48664A) exerts in vitro growth inhibitory effects that are not only related to S-adenosylmethionine decarboxylase (SAMdc) inhibition." Biochim Biophys Acta **1335**(1-2): 144-52.

Ekstrom, J. L., Mathews, II, et al. (1999). "The crystal structure of human S-adenosylmethionine decarboxylase at 2.25 Å resolution reveals a novel fold." Structure Fold Des **7**(5): 583-95.

Ekstrom, J. L., W. D. Tolbert, et al. (2001). "Structure of a human S-adenosylmethionine decarboxylase self-processing ester intermediate and mechanism of putrescine stimulation of processing as revealed by the H243A mutant." Biochemistry **40**(32): 9495-504.

Fairlamb, A. H. and A. Cerami (1992). "Metabolism and functions of trypanothione in the Kinetoplastida." Annu Rev Microbiol **46**: 695-729.

Freifelder, D. (1982). Physical Biochemistry: applications to biochemistry and molecular biology. San Francisco, W.H. Freeman and Co.

Gerner, E. W. and F. L. Meyskens, Jr. (2004). "Polyamines and cancer: old molecules, new understanding." Nat Rev Cancer **4**(10): 781-92.

Gillam, E. M. (2005). "Exploring the potential of xenobiotic-metabolising enzymes as biocatalysts: evolving designer catalysts from polyfunctional cytochrome P450 enzymes." Clin Exp Pharmacol Physiol **32**(3): 147-52.

Gonzalez, N. S., C. Ceriani, et al. (1992). "Differential regulation of putrescine uptake in *Trypanosoma cruzi* and other trypanosomatids." Biochem Biophys Res Commun **188**(1): 120-8.

Hao, J. and A. Berry (2004). "A thermostable variant of fructose biphosphate aldolase constructed by directed evolution also shows increased stability in organic solvents." Protein Eng Des Sel **17**(9): 689-97.

Hoyt, M. A., L. J. Williams-Abbott, et al. (2000). "Cloning and expression of the S-adenosylmethionine decarboxylase gene of *Neurospora crassa* and processing of its product." Mol Gen Genet **263**(4): 664-73.

Janne, J., L. Alhonen, et al. (2004). "Genetic approaches to the cellular functions of polyamines in mammals." Eur J Biochem **271**(5): 877-94.

Jeffress, M. and S. Fields (2005). "Identification of putative *Plasmodium falciparum* mefloquine resistance genes." Mol Biochem Parasitol **139**(2): 133-9.

Jensen-Pergakes, K. L., M. A. Kennedy, et al. (1998). "Sequencing, disruption, and characterization of the *Candida albicans* sterol methyltransferase (ERG6) gene: drug susceptibility studies in *erg6* mutants." Antimicrob Agents Chemother **42**(5): 1160-7.

Kinch, L. N. and M. A. Phillips (2000). "Single-turnover kinetic analysis of *Trypanosoma cruzi* S-adenosylmethionine decarboxylase." Biochemistry **39**(12): 3336-43.

Kinch, L. N., J. R. Scott, et al. (1999). "Cloning and kinetic characterization of the *Trypanosoma cruzi* S-adenosylmethionine decarboxylase." Mol Biochem Parasitol **101**(1-2): 1-11.

Lakowicz, J. R. (1983). Principles of Fluorescence Spectroscopy. New York, Plenum Press.

Laue, T. M., Shah, B., Ridgeway, T.M., and Pelletier, S.L. (1992). Analytical Ultracentrifugation in Biochemistry and Polymer Science. Cambridge, UK, Royal Society of Chemistry.

Lockless, S. W. and R. Ranganathan (1999). "Evolutionarily conserved pathways of energetic connectivity in protein families." Science **286**(5438): 295-9.

Middendorp, O., C. Ortler, et al. (2004). "Yeast growth selection system for the identification of cell-active inhibitors of beta-secretase." Biochim Biophys Acta **1674**(1): 29-39.

- Morozova, L., J. Desmet, et al. (1993). "Complexes of the polyamines spermine, spermidine and putrescine with alpha-lactalbumins." Eur J Biochem **218**(2): 303-9.
- Osterman, A., N. V. Grishin, et al. (1994). "Formation of functional cross-species heterodimers of ornithine decarboxylase." Biochemistry **33**(46): 13662-7.
- Osterman, A. L., H. B. Brooks, et al. (1999). "Lysine-69 plays a key role in catalysis by ornithine decarboxylase through acceleration of the Schiff base formation, decarboxylation, and product release steps." Biochemistry **38**(36): 11814-26.
- Park, S. J. and Y. D. Cho (1999). "Identification of functionally important residues of *Arabidopsis thaliana* S-adenosylmethionine decarboxylase." J Biochem (Tokyo) **126**(6): 996-1003.
- PDR (2005). Physician's Desk Reference, Thomson PDR.
- Pegg, A. E. and P. P. McCann (1992). "S-adenosylmethionine decarboxylase as an enzyme target for therapy." Pharmacol Ther **56**(3): 359-77.
- Peluffo, G., L. Piacenza, et al. (2004). "L-arginine metabolism during interaction of *Trypanosoma cruzi* with host cells." Trends Parasitol **20**(8): 363-9.
- Poso, H., R. Sinervirta, et al. (1975). "S-adenosylmethionine decarboxylase from baker's yeast." Biochem J **151**(1): 67-73.
- Raillard, S., A. Krebber, et al. (2001). "Novel enzyme activities and functional plasticity revealed by recombining highly homologous enzymes." Chem Biol **8**(9): 891-8.
- Reynolds, M. G., J. Oh, et al. (2001). "In vitro generation of novel pyrimethamine resistance mutations in the *Toxoplasma gondii* dihydrofolate reductase." Antimicrob Agents Chemother **45**(4): 1271-7.
- Saab-Rincon, G., V. R. Juarez, et al. (2001). "Different strategies to recover the activity of monomeric triosephosphate isomerase by directed evolution." Protein Eng **14**(3): 149-55.

Schroder, G. and J. Schroder (1995). "cDNAs for S-adenosyl-L-methionine decarboxylase from *Catharanthus roseus*, heterologous expression, identification of the proenzyme-processing site, evidence for the presence of both subunits in the active enzyme, and a conserved region in the 5' mRNA leader." Eur J Biochem **228**(1): 74-8.

Segel, I. (1993). Enzyme Kinetics. New York, John Wiley & Sons, Inc.

Shionyu-Mitsuyama, C., Y. Ito, et al. (2005). "In vitro evolutionary thermostabilization of congerin II: a limited reproduction of natural protein evolution by artificial selection pressure." J Mol Biol **347**(2): 385-97.

Sophianopoulos, J. A., S. J. Durham, et al. (1978). "Ultrafiltration is theoretically equivalent to equilibrium dialysis but much simpler to carry out." Arch Biochem Biophys **187**(1): 132-7.

Stanley, B. A. and A. E. Pegg (1991). "Amino acid residues necessary for putrescine stimulation of human S-adenosylmethionine decarboxylase proenzyme processing and catalytic activity." J Biol Chem **266**(28): 18502-6.

Stanley, B. A., A. E. Pegg, et al. (1989). "Site of pyruvate formation and processing of mammalian S-adenosylmethionine decarboxylase proenzyme." J Biol Chem **264**(35): 21073-9.

Stanley, B. A., L. M. Shantz, et al. (1994). "Expression of mammalian S-adenosylmethionine decarboxylase in *Escherichia coli*. Determination of sites for putrescine activation of activity and processing." J Biol Chem **269**(11): 7901-7.

Stemmer, W. P. (1994). "Rapid evolution of a protein in vitro by DNA shuffling." Nature **370**(6488): 389-91.

Suel, G. M., S. W. Lockless, et al. (2003). "Evolutionarily conserved networks of residues mediate allosteric communication in proteins." Nat Struct Biol **10**(1): 59-69.

Svensson, F., H. Mett, et al. (1997). "CGP 48664, a potent and specific S-adenosylmethionine decarboxylase inhibitor: effects on regulation and stability of the enzyme." Biochem J **322** (Pt 1): 297-302.

- Tarleton, R. L. (2003). "Chagas disease: a role for autoimmunity?" Trends Parasitol **19**(10): 447-51.
- Tekwani, B. L., C. J. Bacchi, et al. (1992). "Irreversible inhibition of S-adenosylmethionine decarboxylase of *Trypanosoma brucei brucei* by S-adenosylmethionine analogues." Biochem Pharmacol **44**(5): 905-11.
- Thomas, T., N. Shah, et al. (1999). "Polyamine biosynthesis inhibitors alter protein-protein interactions involving estrogen receptor in MCF-7 breast cancer cells." J Mol Endocrinol **22**(2): 131-9.
- Tolbert, W. D., J. L. Ekstrom, et al. (2001). "The structural basis for substrate specificity and inhibition of human S-adenosylmethionine decarboxylase." Biochemistry **40**(32): 9484-94.
- Tolbert, W. D., Y. Zhang, et al. (2003). "Mechanism of human S-adenosylmethionine decarboxylase proenzyme processing as revealed by the structure of the S68A mutant." Biochemistry **42**(8): 2386-95.
- Toms, A. V., C. Kinsland, et al. (2004). "Evolutionary links as revealed by the structure of *Thermotoga maritima* S-adenosylmethionine decarboxylase." J Biol Chem **279**(32): 33837-46.
- Toney, M. D. and J. F. Kirsch (1989). "Direct Bronsted analysis of the restoration of activity to a mutant enzyme by exogenous amines." Science **243**(4897): 1485-8.
- Toney, M. D. and J. F. Kirsch (1993). "Lysine 258 in aspartate aminotransferase: enforcer of the Circe effect for amino acid substrates and general-base catalyst for the 1,3-prototropic shift." Biochemistry **32**(6): 1471-9.
- Tye, C. K., G. Kasinathan, et al. (1998). "An approach to use an unusual adenosine transporter to selectively deliver polyamine analogues to trypanosomes." Bioorg Med Chem Lett **8**(7): 811-6.
- Urbina, J. A. and R. Docampo (2003). "Specific chemotherapy of Chagas disease: controversies and advances." Trends Parasitol **19**(11): 495-501.
- van Poelje, P. D. and E. E. Snell (1990). "Pyruvoyl-dependent enzymes." Annu Rev Biochem **59**: 29-59.

Voet, D. a. V., J (1995). Biochemistry. New York, John Wiley & Sons, Inc.

Wallace, H. M. and A. V. Fraser (2004). "Inhibitors of polyamine metabolism: review article." Amino Acids **26**(4): 353-65.

White, W. H., P. L. Gunyuzlu, et al. (2001). "Saccharomyces cerevisiae is capable of de Novo pantothenic acid biosynthesis involving a novel pathway of beta-alanine production from spermine." J Biol Chem **276**(14): 10794-800.

Xiong, H. and A. E. Pegg (1999). "Mechanistic studies of the processing of human S-adenosylmethionine decarboxylase proenzyme. Isolation of an ester intermediate." J Biol Chem **274**(49): 35059-66.

Xiong, H., B. A. Stanley, et al. (1999). "Role of cysteine-82 in the catalytic mechanism of human S-adenosylmethionine decarboxylase." Biochemistry **38**(8): 2462-70.

Xiong, H., B. A. Stanley, et al. (1999). "Role of cysteine-82 in the catalytic mechanism of human S-adenosylmethionine decarboxylase." Biochemistry **38**(8): 2462-70.

Xiong, H., B. A. Stanley, et al. (1997). "Processing of mammalian and plant S-adenosylmethionine decarboxylase proenzymes." J Biol Chem **272**(45): 28342-8.

Yakubu, M. A., S. Majumder, et al. (1993). "Inhibition of S-adenosyl-L-methionine (AdoMet) decarboxylase by the decarboxylated AdoMet analog 5'-[(Z)-4-amino-2-butenyl]methylamino)-5'-deoxyadenosine (MDL 73811) decreases the capacities of Trypanosoma cruzi to infect and multiply within a mammalian host cell." J Parasitol **79**(4): 525-32.

Zappia, V., M. Carteni-Farina, et al. (1972). "S-adenosylmethionine decarboxylase from human prostate. Activation by putrescine." Biochem J **129**(3): 703-9.

Zhang, J. H., G. Dawes, et al. (1997). "Directed evolution of a fucosidase from a galactosidase by DNA shuffling and screening." Proc Natl Acad Sci U S A **94**(9): 4504-9.

VITA

Tracy Clyne Beswick was born in Clinton, Oklahoma on December 8, 1976 to her parents Bob and Randy Clyne. Upon graduation from Edmond Memorial High School in 1995, Tracy entered Abilene Christian University where she earned a Bachelor of Science degree in Biochemistry in 1999. Tracy then entered the Graduate Program in Molecular Biophysics at the University of Texas Southwestern Medical Center at Dallas in 1999, working in Dr. Meg Phillips' lab. Three years into her Ph.D. training, Tracy was accepted to the Medical Scientist Training Program at the University of Texas Southwestern Medical Center at Dallas. She left the lab for a year to complete the first year of medical school. Tracy returned to the lab for 2 years to finish her research, during which time she married Christopher Sean Beswick. She will earn her Ph.D. in Molecular Biophysics from the University of Texas Southwestern Medical Center at Dallas in July, 2005.

Permanent Address: 3719 Matson Street

Fort Worth, TX 76117